Spleen tyrosine kinase (SYK) blocks autophagic Tau degradation *in vitro* and *in vivo*

Received for publication, February 14, 2019, and in revised form, July 12, 2019 Published, Papers in Press, July 19, 2019, DOI 10.1074/jbc.RA119.008033

Jonas Elias Schweig[‡§¶1], Hailan Yao[‡¶], Kyle Coppola[‡¶], Chao Jin[‡], Fiona Crawford[‡§¶], Michael Mullan[‡§], and Daniel Paris[‡§¶]

From the [‡]Roskamp Institute, Sarasota, Florida 34243, [§]The Open University, Milton Keynes MK7 6AA, United Kingdom, and the [¶]James A. Haley Veterans Hospital, Tampa, Florida 33612

Edited by Luke O'Neill

Spleen tyrosine kinase (SYK) plays a major role in inflammation and in adaptive immune responses and could therefore contribute to the neuroinflammation observed in various neurodegenerative diseases. Indeed, previously we have reported that SYK also regulates β-amyloid (Aβ) production and hyperphosphorylation of Tau protein involved in these diseases. Moreover, SYK hyperactivation occurs in a subset of activated microglia, in dystrophic neurites surrounding Aβ deposits, and in neurons affected by Tau pathology both in individuals with Alzheimer's disease (AD) and in AD mouse models. SYK activation increases Tau phosphorylation and accumulation, suggesting that SYK could be an attractive target for treating AD. However, the mechanism by which SYK affects Tau pathology is not clear. In this study, using cell biology and biochemical approaches, along with immunoprecipitation and immunoblotting, quantitative RT-PCR, and ELISAs, we found that SYK inhibition increases autophagic Tau degradation without impacting Tau production. Using neuron-like SH-SY5Y cells, we demonstrate that SYK acts upstream of the mammalian target of rapamycin (mTOR) pathway and that pharmacological inhibition or knockdown of SYK decreases mTOR pathway activation and increases autophagic Tau degradation. Interestingly, chronic SYK inhibition in a tauopathy mouse model profoundly reduced Tau accumulation, neuroinflammation, neuronal and synaptic loss, and also reversed defective autophagy. Our results further suggest that the SYK up-regulation observed in the brains of individuals with AD contributes to defective autophagic clearance leading to the accumulation of pathogenic Tau species. These findings further highlight SYK as a therapeutic target for the treatment of tauopathies and other neurodegenerative proteinopathies associated with defective autophagic clearance.

Alzheimer's disease (AD)[2] is the most prevalent form of dementia and is characterized by the pathological accumulation of Tau and Aβ aggregates. Protein misfolding, aggregation, and accumulation constitute a pathological hallmark of neurodegenerative proteinopathies. Many studies have suggested that neurodegeneration is, at least partly, caused by a dysfunctional degradation of proteins that are prone to aggregate. In fact, an impaired autophagic clearance of macromolecules has been widely accepted to be a major contributor to various neurodegenerative diseases (1–4) by promoting the accumulation of misfolded proteins. The mammalian target of rapamycin (mTOR) is known to regulate autophagy (5). The members of the mTOR pathway, including phosphatidylinositol-4,5-bisphosphate 3-kinase (PI3K), 3-phosphoinositide-dependent protein kinase 1 (PDK1), protein kinase B (Akt), tuberous sclerosis 1/2 (TSC1/2), Ras homolog-enriched in brain (Rheb), mTOR, and ribosomal protein S6 kinase (S6K), thereby also indirectly control the autophagic degradation of proteins. AD and frontotemporal lobar degeneration (FTLD) share the accumulation of Tau as a common underlying pathology. In human AD and FTLD cases, as well as in mouse models of AD and pure tauopathy, autophagy has been found to be decreased (6–8) and to contribute to the pathological accumulation of Tau aggregates. Impaired autophagy has been linked to an overactive mTOR pathway, which acts as a regulator of autophagy initiation and lysosomal degradation, thereby controlling the autophagic flux (5, 9).

More specifically, in the frontotemporal dementia and parkinsonism linked to chromosome 17 (FTDP-17) mouse model that overexpresses mutant Tau (Tg Tau P301S), direct inhibition of mTOR with either rapamycin or temsirolimus attenuated Tau pathology (10, 11). Furthermore, stimulation of autophagy by trehalose or by the overexpression of the transcription factor EB were both shown to be efficient in reducing neurodegeneration and mitigating tauopathy in Tg Tau P301S mice (12, 13) suggesting that inhibiting mTOR may have therapeutic value for the treatment of tauopathies.

The nonreceptor spleen tyrosine kinase (SYK) is known as a modulator of the immune response. SYK has been shown to be involved in B-cell receptor and T-cell receptor signaling. Hence, SYK inhibition has been proposed as a therapeutic

This work was supported in part by the Department of Veterans Affairs VA Merit Award 1I01BX002572 (to F. C.) and the Roskamp Foundation. The authors declare that they have no conflicts of interest with the contents of this article.

This article contains Fig. S1.

[1] To whom correspondence should be addressed: Roskamp Institute, 2040 Whitfield Ave., Sarasota, FL 34243. Tel.: 941-752-2949; Fax: 941-752-2948; E-mail: jschweig@roskampinstitute.net.

[2] The abbreviations used are: AD, Alzheimer's disease; CQ, chloroquine; ANOVA, analysis of variance; PI3K, phosphatidylinositol 3-kinase; BAY61, BAY61-3606; Tg, transgenic; SYK, spleen tyrosine kinase; Aβ, β-amyloid; mTOR, mammalian target of rapamycin; qPCR, quantitative PCR; S6K, ribosomal protein S6 kinase; FTLD, frontotemporal lobar degeneration; IP, immunoprecipitation; GFAP, glial fibrillary acidic protein; iNOS, inducible nitric-oxide synthase; IL, interleukin; BDNF, brain-derived neurotrophic factor; PMSF, phenylmethylsulfonyl fluoride.

approach for various diseases, including leukemia, autoimmune disorders, and allergies (14–17).

SYK has also been suggested to phosphorylate microtubules in B-cells (18) and to be involved in neuron-like differentiation and extracellular signal-regulated kinase (ERK) activation in embryonal carcinoma P19 cells (19). Furthermore, pharmacological SYK inhibition has been found to stabilize microtubules in paclitaxel-resistant tumor cells (20).

SYK has been shown to mediate the activation of microglial cells induced by Aβ oligomers (21, 22), whereas SYK inhibition has been shown to prevent Aβ-mediated neurotoxicity *in vitro* (21). A subsequent study also demonstrated that SYK was the mediator of the Aβ-induced elevated cytokine production, including interleukin 1β (IL-1β) and tumor necrosis factor α (TNFα) which is responsible for increased iNOS expression resulting in apoptosis in primary mouse neuronal cultures (23). In addition, it has been suggested that SYK contributes to microglial dysfunction in AD (24).

In our previous studies, we identified SYK as a novel target for the treatment of AD (25, 26). We found that SYK inhibition can decrease Aβ production and Tau hyperphosphorylation *in vitro* and *in vivo* in mouse models of AD and tauopathy following an acute treatment (25), in part, by promoting the phosphorylation of GSK-3β at the inhibitory Ser-9 site and reducing BACE-1 expression (25).

More recently, we have shown that SYK activation, as measured by p-SYK (Tyr-525/526) levels, is largely increased in dystrophic neurites and microglia of Aβ-overexpressing mouse models of AD (Tg PS1/APPsw, Tg APPsw) and in neurons of a mouse model of tauopathy (Tg Tau P301S) displaying pathological Tau species, whereas the neurons of WT animals showed no activation of SYK (26), suggesting that SYK plays a key role in the formation of AD pathological lesions. Similarly, we observed an increased SYK activation in dystrophic neurites and in neurons affected by the Tau pathology in human AD specimens (26). Interestingly, we have shown that SYK activation promotes Tau accumulation but does not affect Tau expression suggesting that SYK may affect Tau clearance (26). In this study, we further investigated the SYK molecular mechanisms that drive Tau accumulation both *in vitro* and *in vivo*. We show that SYK is a key regulator of the mTOR pathway and that SYK inhibition, as well as suppression of SYK expression, leads to an inhibition of the mTOR pathway, resulting in increased autophagic Tau degradation. Moreover, we show that chronic SYK inhibition lowers pathological Tau accumulation in Tg Tau P301S mice by inhibiting hyperactive mTOR. Furthermore, chronic SYK inhibition reduces the levels of pro-inflammatory cytokines and neuronal and synaptic loss and improves locomotor deficits in Tg Tau P301S mice. These data not only provide further evidence for an important role of SYK in the pathogenesis of AD and the development of tauopathies but also illustrate that pharmacological SYK inhibition may represent a promising therapeutic strategy for the treatment of AD and other neurodegenerative proteinopathies associated with a defective autophagic clearance of misfolded proteins.

Results

Our previous data suggest that SYK may regulate Tau clearance since we have observed that SYK up-regulation promotes Tau accumulation without affecting Tau expression (26). As Tau clearance is known to be regulated via autophagy, we therefore investigated the possible impact of SYK inhibition on the mTOR pathway and autophagic degradation of Tau in SH-SY5Y cells.

SYK inhibition decreases p-Tau, as well as total Tau levels, and reverses the effects of the Akt activator SC79 on the mTOR pathway

We show that SYK inhibition using the selective SYK inhibitor BAY61-3606 (BAY61) (27) dose-dependently decreases p-Tau (Ser-396/404) levels (Fig. 1, *A* and *B*) and total Tau levels in SH-SY5Y cells (Fig. 1, *A* and *B*).

In parallel with the reduction of total Tau levels induced by SYK inactivation with BAY61, a dose-dependent inhibition of several members of the mTOR pathway was observed (Fig. 1, *B* and *C*). Compared with untreated control cells, p-Akt (Ser-473) and p-S6K (Thr-389 and Thr-412) levels were significantly lower following SYK inhibition (Fig. 1*C*, $p < 0.01$). As expected, the Akt activator SC79 stimulated the mTOR pathway, as it increases the phosphorylation levels of p-S6K (Thr-389 and Thr-412) and p-mTOR (Ser-2448) significantly (Fig. 1*C*, $p < 0.01$). We show that SYK inhibition reverses the effects of the Akt activator and decreases the phosphorylation levels of p-Akt (Ser-473), p-S6K (Thr-389 and Thr-412), and p-mTOR (Ser-2448) induced by SC79 (Fig. 1*C*, $p < 0.001$). Interestingly, baseline levels of mTOR phosphorylation remained unchanged following SYK inhibition, but elevated mTOR phosphorylation following SC79 activation was brought back to baseline levels following SYK inhibition, suggesting that SYK inhibition can antagonize dysregulated mTOR phosphorylation (Fig. 1*C*). In addition, we have differentiated SH-SY5Y cells with retinoic acid and BDNF, as described previously by Encinas *et al.* (28), and assessed the effects of SYK inhibition on the Tau level and on the mTOR/autophagy pathway. We show that SYK inhibition with BAY61-3606 also results in decreased total Tau, p-AKT, p-S6K, and p-mTOR levels in differentiated SH-SY5Y cells (Fig. S1*B*), confirming the data obtained with undifferentiated SH-SY5Y cells.

SYK inhibition reverses the effects of the mTOR activator MHY1485 and mimics the effects of the mTOR inhibitor KU0063794

We further investigated the effects of SYK inhibition on the mTOR pathway and determined whether SYK inhibition can overcome the impact of the mTOR activator MHY1485. We also tested the effects of the mTOR inhibitor KU0063794 on phosphorylated and total Tau levels in SH-SY5Y cells to determine whether direct mTOR inactivation can mimic the effects of SYK inhibition. mTOR activation with MHY1485 significantly increased p-mTOR (Ser-2448), p-S6K (Thr-389 and Thr-412), and p-Tau (Ser-396/404) levels, whereas mTOR inhibition with KU0063794 significantly decreased p-Akt (Ser-473), p-S6K (Thr-389 and Thr-412), and p-mTOR (Ser-2448) levels compared with the untreated control cells (Fig. 2, *A* and

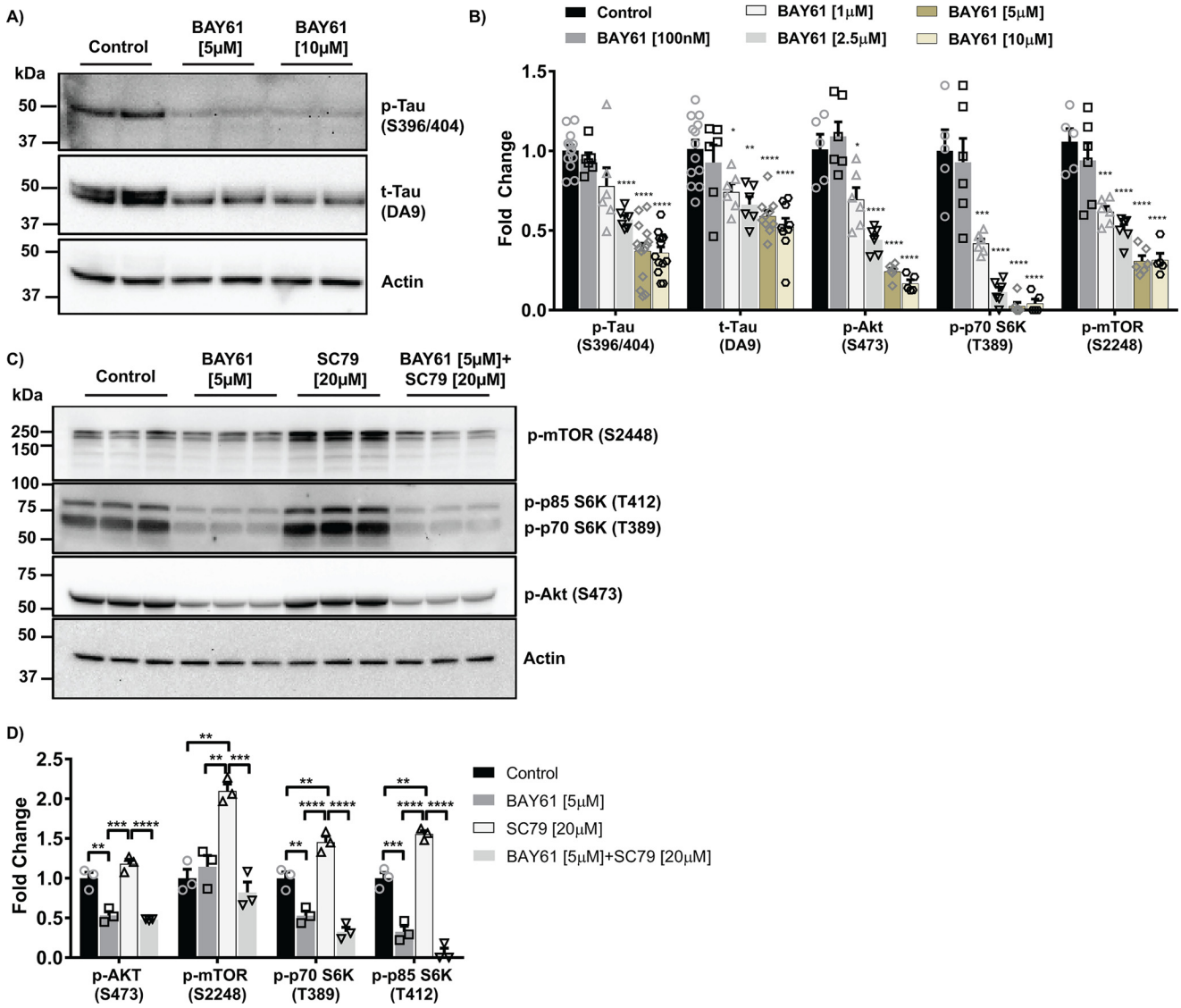

Figure 1. SYK inhibition decreases p-Tau as well as total Tau levels and reverses the effects of the Akt activator SC79 on the mTOR pathway. *A,* representative Western blottings depicting p-Tau (Ser-396/404) and total Tau are shown. Western blot chemiluminescent signals were quantified by densitometry and normalized to actin. *B,* histogram represents the quantification of Western blottings probed with antibodies against p-Tau (Ser-396/404), t-Tau, p-Akt (Ser-473), p-p70S6K (Thr-389), p-mTOR (Ser-2448), normalized to actin, following a 24-h treatment of SH-SY5Y cells with 100 nM and 1, 2.5, 5, or 10 μM of the SYK inhibitor BAY61. ANOVA with post hoc Bonferroni test revealed significant decreases starting at 1 μM. *C,* representative Western blottings depicting p-mTOR (Ser-2448), p-S6K (Thr-389 and Thr-412), and p-Akt (Ser-473) are shown. Western blot chemiluminescent signals were quantified by densitometry and normalized to actin. *D,* histogram represents the quantification of p-mTOR (Ser-2448), p-S6K (Thr-389 and Thr-412), and p-Akt (Ser-473) following a 24-h treatment of SH-SY5Y cells with 5 μM of the SYK inhibitor BAY61-3606 and 20 μM of the Akt activator SC79 and a combination thereof. ANOVA with post hoc Bonferroni test revealed significantly decreased p-Akt (Ser-473) ($p < 0.01$) and p-S6K (Thr-389 and Thr-412) ($p < 0.01$, $p < 0.001$) levels following SYK inhibition ($n = 3$) and also significantly increased p-mTOR (Ser-2448) ($p < 0.01$) and p-S6K (Thr-389 and Thr-412) ($p < 0.01$) levels following Akt activation. SYK inhibition reverses these effects significantly in the double treatment ($n = 3$ for each treatment condition).

B). The levels of t-Tau and p-Tau (Ser-396/404) were also significantly lower in cells that were treated with the mTOR inhibitor than in cells that were treated with the mTOR activator (Fig. 2, *A* and *B*). In fact, mTOR inhibition appears to be mimicking the effects of SYK inhibition on the mTOR pathway (Figs. 1 and 2). Interestingly, SYK inhibition was able to antagonize the increased p-Tau (Ser-396/404), p-S6K (Thr-389 and Thr-412), p-mTOR (Ser-2448), and p-Akt (Ser-473) levels induced by MHY1485 (Fig. 2, *C* and *D*). A trend for an increase in total Tau levels was observed following 24 h of treatment with the mTOR activator MHY1485, which was also prevented by SYK inhibition (Fig. 2, *C* and *D*) showing that SYK inhibition can overcome the effects of a stimulation of the mTOR pathway. Interestingly, SYK inhibition prevents the stimulation of mTOR by the mTOR activator MHY1485 due to the mechanism of action of MHY1485. In fact, MHY1485 facilitates the phosphorylation of mTOR at Ser-2448 by AKT (29) and therefore requires AKT to be active to allow mTOR activation (30). We show that SYK inhibition prevents PI3K/AKT signaling and suppresses mTOR phosphorylation at Ser-2448. Therefore, when SYK is inhibited, AKT is also suppressed and cannot phosphorylate mTOR even in the presence of MHY1485. We observed a greater inhibition of S6K phosphorylation than an inhibition of mTOR phosphorylation with BAY61. This could be explained by the fact that SYK can stimulate JNK, whereas SYK inhibition also reduces JNK (31, 32). It has to be noted that

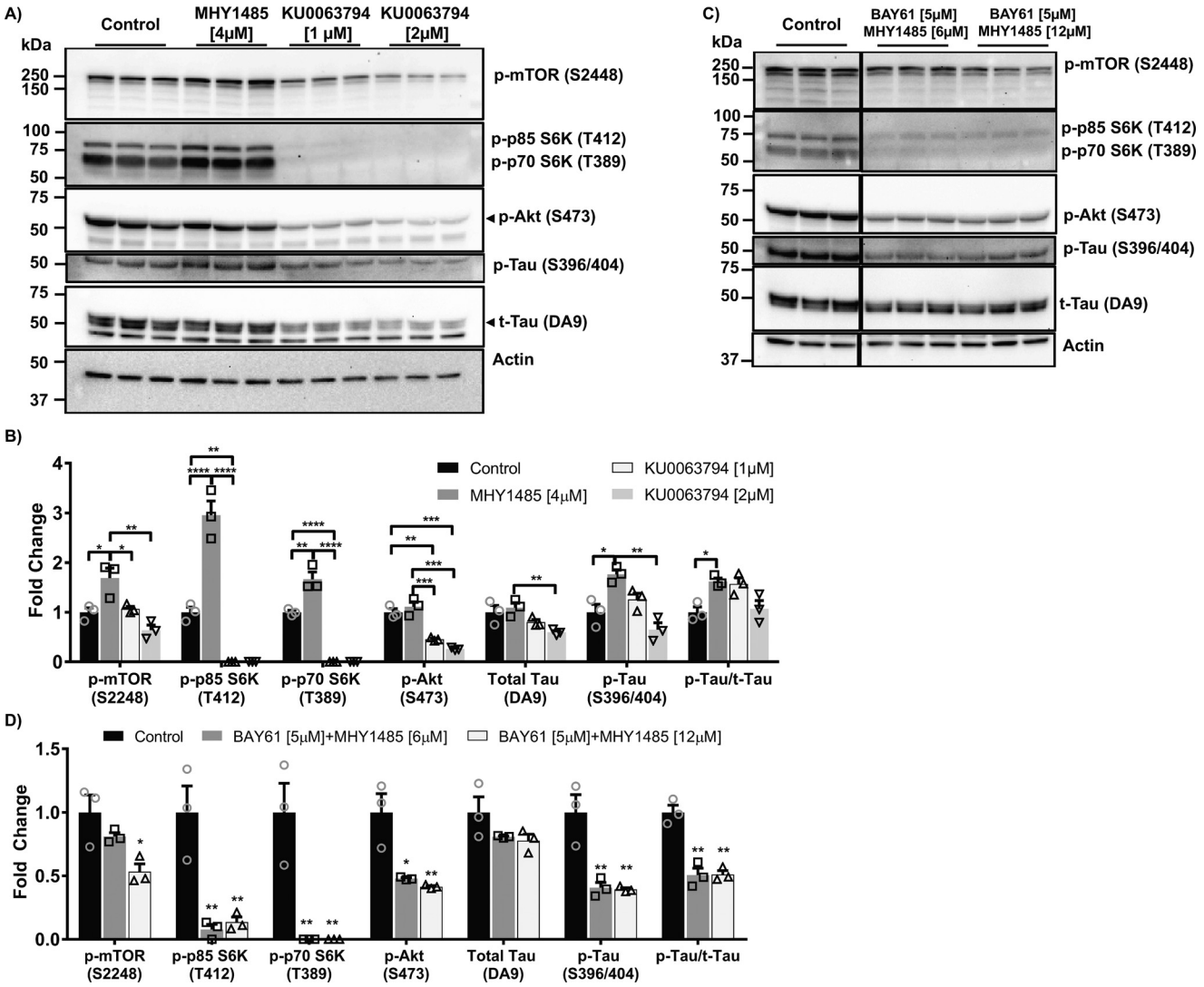

Figure 2. SYK inhibition reverses the effects of the mTOR activator MHY1485 and mimics the effects of the mTOR inhibitor KU0063794. SH-SY5Y cells were treated for 24 h with 4 μM of the mTOR activator MHY1485 or 1–2 μM of the mTOR inhibitor KU0063794 (*A* and B) or a combination of 6–12 μM of the mTOR activator MHY1485 and 5 μM of the SYK inhibitor BAY61-3606 (*C* and *D*). *A,* representative Western blottings depicting p-mTOR (Ser-2448), p-S6K (Thr-389 and Thr-412), p-Akt (Ser-473), p-Tau (Ser-396/404), and t-Tau are shown. *B,* Western blot chemiluminescent signals were quantified by densitometry, normalized to actin, and presented as histograms. ANOVA with post hoc Bonferroni test revealed significantly increased p-mTOR (Ser-2448) ($p < 0.05$), p-S6K (Thr-389 and Thr-412) ($p < 0.01$, $p < 0.0001$), and p-Tau (Ser-396/404) ($p < 0.05$) levels compared with untreated control cells following mTOR activation by MHY1485, whereas mTOR inhibition by KU0063794 decreased p-S6K (Thr-389 and Thr-412) ($p < 0.0001$ and $p < 0.01$) and p-Akt (Ser-473) ($p < 0.01$) levels significantly compared with control ($n = 3$ for each treatment condition). *C,* representative Western blottings depicting p-mTOR (Ser-2448), p-S6K (Thr-389 and Thr-412), p-Akt (Ser-473), p-Tau (Ser-396/404) ,and t-Tau are shown. *D,* Western blot chemiluminescent signals were quantified by densitometry, normalized to actin, and presented as histograms. ANOVA with post hoc Bonferroni test revealed that the combination of the mTOR activator and the SYK inhibitor results in significantly decreased p-mTOR (Ser-2448) ($p < 0.01$), p-S6K (Thr-389 and Thr-412) ($p < 0.01$), p-Akt (Ser-473) ($p < 0.01$), and p-Tau (Ser-396/404) ($p < 0.01$) levels compared with untreated control cells ($n = 3$ for each treatment condition).

JNK can also directly phosphorylate S6K (33) and also affects the degradation of S6K. Therefore, the effects that we are observing on S6K phosphorylation could be mediated by the combined suppression of JNK and mTOR following SYK inhibition, thus explaining why overall SYK inhibition has a greater impact on S6K phosphorylation than on mTOR phosphorylation. We also observed an inhibition of Akt following mTOR inhibition with KU0063794. The effect of the mTOR inhibitor KU0063794 on Akt phosphorylation is expected and has been described before (34). In fact, Akt (Ser-473) is a known substrate of mTOR, and mTOR has been shown to regulate Akt phosphorylation at that site (35–38).

In addition, we show that mTOR inhibition with KU0063794 significantly decreases p-Tau (Ser-396/404) and t-Tau levels in SH-SY5Y cells stably overexpressing SYK (Fig. S1) that exhibit increased Tau levels compared with control cells (26). These data suggest that mTOR inhibition can overcome the impact of SYK up-regulation on t-Tau levels. In summary, these results show that SYK inhibition and direct mTOR inhibition have similar effects on the mTOR pathway and Tau levels. Furthermore, SYK inhibition can reverse the effects of mTOR activation on members of the mTOR pathway and Tau, thereby underlining a role of SYK as an upstream modulator of the mTOR pathway and regulator of autophagic Tau degradation.

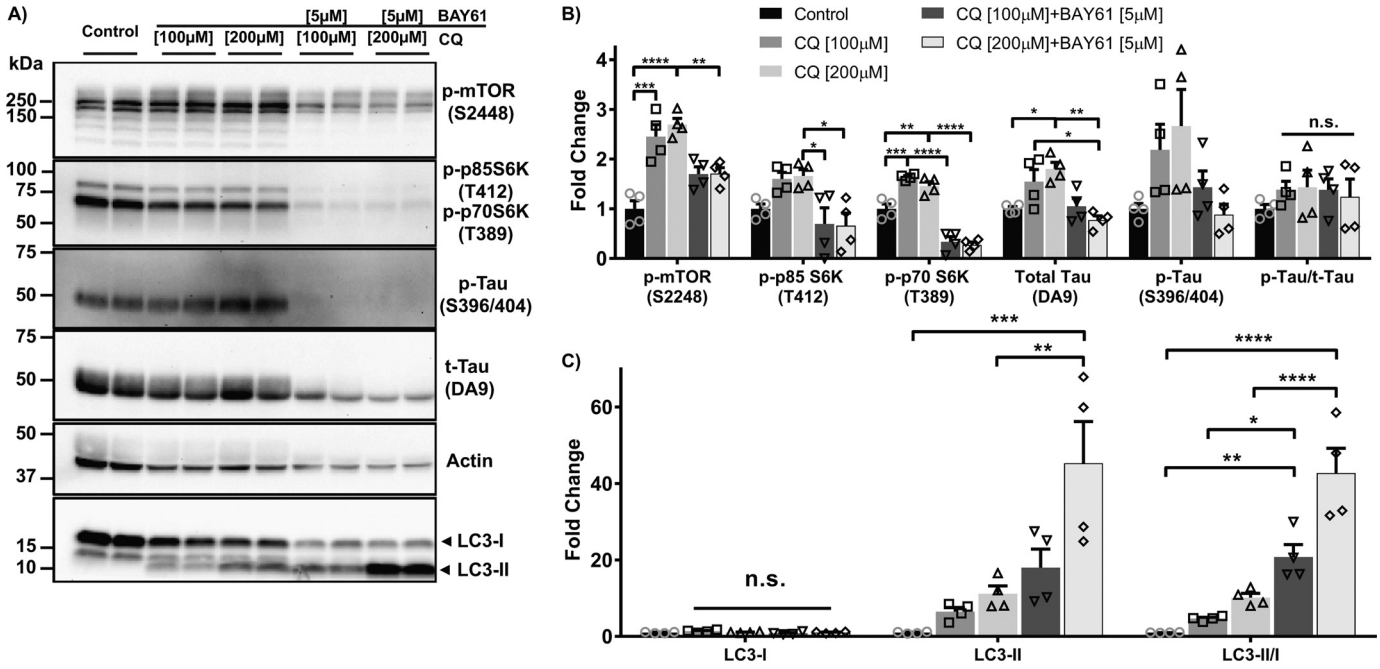

Figure 3. SYK inhibition increases the autophagic flux and decreases tau levels in the presence of the lysosomal inhibitor chloroquine. SH-SY5Y cells were treated for 24 h with 100–200 μM of the lysosomal inhibitor chloroquine (CQ) or a combination of 100–200 μM CQ and 5 μM of the SYK inhibitor BAY61-3606. *A,* representative Western blottings depicting p-mTOR (Ser-2448), p-S6K (Thr-389 and Thr-412), p-Tau (Ser-396/404), t-Tau, and LC3-I/II are shown. *B* and C, Western blot chemiluminescent signals were quantified by densitometry, normalized to actin, and presented as histograms. *B,* ANOVA with post hoc Bonferroni test revealed significantly increased p-mTOR (Ser-2448) ($p < 0.001$), p-S6K (Thr-389) ($p < 0.001$), and t-Tau ($p < 0.05$) levels compared with untreated control cells following lysosomal inhibition by CQ, whereas a combination of CQ and the SYK inhibitor reverses the effects of CQ, leading to significantly decreased p-mTOR (Ser-2448) ($p < 0.01$), p-S6K (Thr-389 and Thr-412) ($p < 0.0001$, $p < 0.05$), and t-Tau ($p < 0.01$) levels compared with CQ alone ($n = 4$ for each treatment condition). *C,* ANOVA with post hoc Bonferroni test revealed that the combination of the lysosomal and the SYK inhibitor results in significantly increased autophagic flux compared with CQ alone (CQ (100 μM) + BAY61, $p < 0.05$, CQ (200 μM) + BAY61, $p < 0.0001$), as measured by LC3II/I, whereas the LC3-I levels were not altered significantly (*n.s.*) ($n = 4$ for each treatment condition).

SYK inhibition increases the autophagic flux and decreases Tau levels in the presence of the lysosomal inhibitor chloroquine

Having shown that SYK acts upstream of mTOR and thereby influences the autophagic degradation of Tau, we investigated whether SYK inhibition could impact the autophagic flux by quantifying the amount of the microtubule-associated protein 1A/1B-light chain (LC3). During autophagy initiation, soluble cytosolic LC3-I gets lipidated, and the resulting LC3-II becomes associated with the inside and outside of autophagosomal membranes (39). After the fusion of autophagosomes with lysosomes, LC3-II is degraded. Hence, the ratio of unlipidated LC-I to lipidated LC3-II can be used to measure the autophagic flux, the rate of autophagy initiation, and lysosomal degradation (40, 41). Because an increase in LC3-II levels following drug treatment could be indicative of either an increase in autophagy initiation or a decrease in lysosomal degradation, we employed a lysosome inhibitor (chloroquine (CQ)) to determine the rate of autophagy initiation, as described previously (40, 42). CQ accumulates in the lysosomes and raises their pH. Thereby, CQ decreases the functionality of lysosomal proteases and inhibits the fusion of lysosomes and autophagosomes. Therefore, CQ allows the observation of the conversion rate of LC3-I to LC3-II (autophagy initiation) by limiting the degradation of LC3-II. We treated SH-SY5Y cells for 24 h with two different doses of CQ (100 and 200 μM) alone or in combination with 5 μM of the SYK inhibitor BAY61. CQ treatment significantly increased p-S6K (Thr-389), p-mTOR (Ser-2448), and t-Tau levels (Fig. 3, *A* and *B*) showing an inhibition of lysosomal t-Tau degradation. As expected, CQ treatment also increased the ratio of LC3-II/I by decreasing the degradation of LC3-II (Fig. 3*C*). Importantly, the increased levels of p-S6K (Thr-389), p-mTOR (Ser-2448), and t-Tau levels induced by CQ were significantly reduced following SYK inhibition (Fig. 3, *A* and *B*). The ratio of LC3II/I was further increased after a double treatment with CQ and BAY61 compared with CQ alone (Fig. 3*C*). Because the degradation of LC3-II is inhibited by CQ, the additional increase of LC3-II observed in cells treated with CQ and the SYK inhibitor suggests that SYK inhibition accelerates the conversion of LC3-I into LC3-II and therefore stimulates the autophagic flux. The increased degradation of t-Tau following the co-treatment with CQ and the SYK inhibitor compared with CQ alone (Fig. 3) suggests that SYK inhibition not only increases autophagy initiation but may also increase the lysosomal degradation of Tau, which was antagonized by CQ.

SYK inhibition does not affect Tau translation or transcription

Because SYK acts upstream of the mTOR pathway and the downstream kinase S6K is known to be involved in translation, we investigated whether SYK inhibition and S6K inhibition could impact Tau translation (Fig. 4). We show that the reduction in t-Tau protein level following SYK inhibition is not caused by a reduction of t-Tau transcription as measured by

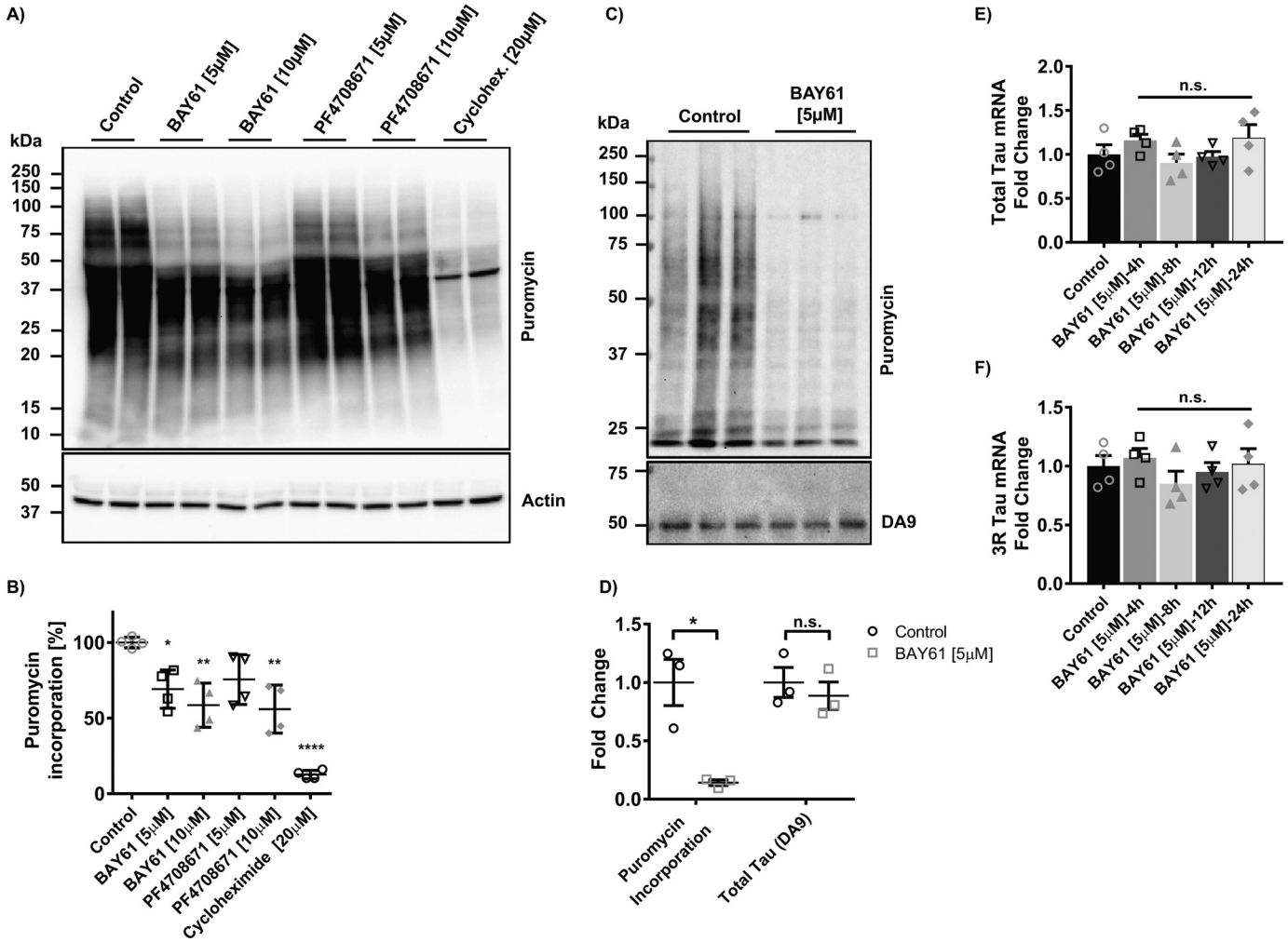

Figure 4. SYK inhibition does not alter transcription or translation levels of Tau *in vitro*. *A* and *B*, SUrface SEnsing of Translation (SUnSET) technique (43) was used to assess the impact of SYK inhibition on protein translation. SH-SY5Y cells were treated with 5–10 μM of the SYK inhibitor BAY61-3606 or 5–10 μM of the S6K inhibitor PF4708671 for 24 h or with cycloheximide for 5 h. Cells were then treated for 1 h with 10 μg/ml puromycin. Levels of newly synthesized proteins containing puromycin were then detected by Western blotting using an anti-puromycin antibody. *A*, representative Western blottings depicting puromycin and actin are shown. *B*, Western blot chemiluminescent signals were quantified by densitometry, normalized to actin, and presented as histograms. ANOVA with post hoc Bonferroni test revealed total levels of translation are significantly reduced following SYK inhibition (5 μM $p < 0.05$; 10 μM $p < 0.01$) or S6K inhibition (10 μM $p < 0.01$) or following cycloheximide treatment (20 μM $p < 0.0001$) ($n = 4$ for each treatment condition). *C* and *D*, anti-puromycin antibodies and protein A-magnetic beads were used for immunoprecipitation of the cell lysate following treatment with 5 μM BAY61. Western blotting analysis with anti-puromycin and anti-t-tau antibodies, quantification (as in *A* and *B*) and subsequent unpaired *t* test (*D*) revealed no significant difference in total tau translation levels following SYK inhibition, whereas the puromycin levels were significantly decreased ($p < 0.05$) ($n = 3$ for each treatment condition). *E* and *F*, mRNA levels of total Tau and 3R Tau were measured by RT-PCR following different durations of treatment with 5 μM of the SYK inhibitor BAY61-3606. ANOVA with post hoc Bonferroni test revealed no significant difference of tau mRNA levels treated with BAY61-3606 for 4, 8, 12, or 24 h *versus* untreated control ($n =$ 4 for each treatment condition).

RT-PCR (mRNA) (Fig. 4). We then assessed protein translation in SH-SY5Y cells that were treated for 24 h with either 5 or 10 μM of the SYK inhibitor BAY61 or 5 or 10 μM of the S6K inhibitor PF4708671 or 20 μM cycloheximide (inhibitor of protein translation used as a positive control) (Fig. 4*A*). Protein translation was quantified using the SUrface SEnsing of Translation (SUnSET) techniques (43) by monitoring puromycin incorporation in newly-synthesized proteins. Both SYK inhibition and S6K inhibition significantly decreased puromycin incorporation, particularly in proteins of higher molecular weight (Fig. 4*A*). This may suggest a general effect of SYK inhibition on translation that is possibly mediated by S6K inhibition, because SYK inhibition completely prevents S6K phosphorylation and because a direct S6K inhibition mimics the impact of SYK inhibition on protein translation (Fig. 4, *A* and *B*). However, isolation of newly synthesized proteins by immunoprecipitation using an anti-puromycin antibody followed by Western blot analysis using a total Tau antibody (DA9) to quantify the amount of nascent Tau reveals no impact of SYK inhibition (Fig. 4, *C* and *D*) on Tau protein translation. In addition, t-Tau and 3R mRNA levels in SH-SY5Y cells are not impacted by SYK inhibition with 5 μM BAY61 for 4, 8, 12, and 24 h (Fig. 4, *E* and *F*) showing that SYK inhibition does not affect Tau expression at the mRNA level. These data further demonstrate that the decrease in t-Tau level, observed following SYK inhibition, is mainly caused by an increase in autophagic Tau degradation, rather than a decreased level of Tau translation or transcription.

In a subsequent experiment, we tested the effects of S6K inhibition by PF4708671 on the mTOR pathway and Tau degrada-

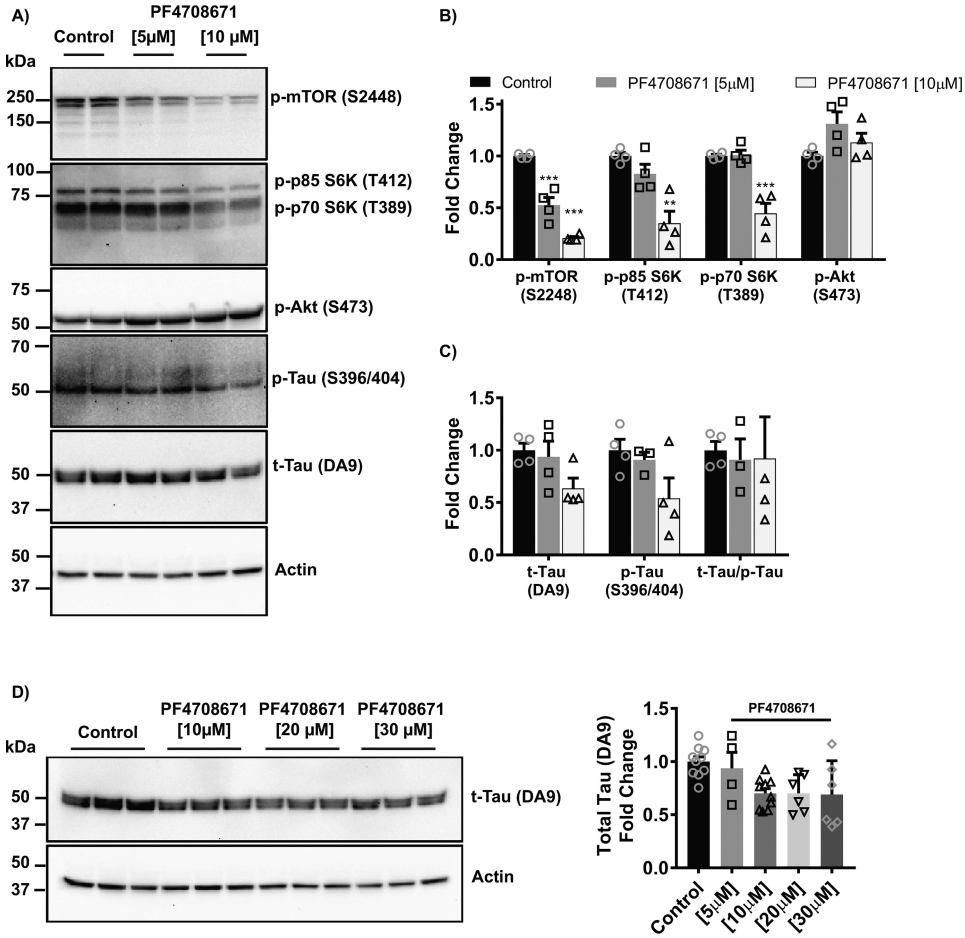

Figure 5. S6K inhibition by PF4708671 has similar effects as SYK inhibition on the mTOR pathway and tau levels. SH-SY5Y cells were treated for 24 h with 5–10 μM of the S6K inhibitor PF4708671. Western blottings were quantified, normalized to actin, and expressed relative to the untreated control cells. *A,* representative Western blottings depicting p-mTOR (Ser-2448), p-S6K (Thr-389 and Thr-412), p-Akt (Ser-473), p-Tau (Ser-396/404), and t-Tau are shown. *B* and *C*, Western blot chemiluminescent signals were quantified by densitometry, normalized to actin, and presented as histograms. *B,* ANOVA and post hoc Bonferroni test revealed that p-mTOR (Ser-2448) ($p < 0.001$) and p-S6K (Thr-389 and Thr-412) ($p < 0.001$, $p < 0.01$) levels were reduced significantly compared with control following S6K inhibition. p-Akt levels remained unchanged. *C,* total Tau and p-Tau (Ser-396/404) were slightly reduced at the highest dose of PF4708671 ($n = 4$ for each treatment condition). *D,* representative Western blottings and quantification thereof depicting the fold change of t-Tau following treatment with 20 and 30 μM of the S6K inhibitor PF4708671.

tion. S6K inhibition using 10 μM PF4708671 leads to significant reduction in p-mTOR (Ser-2448) and p-S6K (Thr-389 and Thr-412) levels (Fig. 5, *A* and *B*). p-Akt (Ser-473) levels remain unchanged following S6K inhibition. This could imply the existence of a feedback mechanism following S6K inhibition on the mTOR pathway, as S6K is a downstream kinase of mTOR. In fact, S6K has been shown to phosphorylate mTOR (Ser-2448) (44), and the reductions in mTOR phosphorylation that we observed with PF4708671 are consistent with that observation. A nonsignificant trend for a decrease p-Tau (Ser-396/404) and t-Tau levels was observed in SH-SY5Y cells (Fig. 5, *A* and *C*) following 24 h of treatment with the S6K inhibitor suggesting that the S6K inhibition observed following SYK inactivation does not play a major role in the increased Tau clearance induced by SYK inhibition.

In summary, these *in vitro* data show an upstream modulatory role of SYK on the mTOR pathway in SH-SY5Y cells and suggest that SYK is a major kinase that regulates the autophagic degradation of Tau. Our data suggest that SYK inhibition increases Tau degradation in SH-SY5Y cells by inhibiting the mTOR pathway and increasing the autophagic flux.

Suppression of SYK expression mimics pharmacological inhibition of SYK and decreases total Tau levels

To validate the data obtained following pharmacological inhibition of SYK with BAY61 and to ensure that the effects observed were mediated by SYK inhibition, we knocked down SYK by stably overexpressing a SYK shRNA in SH-SY5Y cells. As expected, a significant decrease in total SYK (t-SYK) (Fig. 6) was observed in the SYK knockdown SH-SY5Y cells compared with control SH-SY5Y cells that were stably transfected with a nonsense shRNA using the same vector. We show that SYK knockdown significantly decreases p-mTOR (Ser-2448), p-S6K (Thr-389), p-Akt (Ser-473), p-Tau (Ser-396/404) , and t-Tau levels (Fig. 6, *A* and *B*) mimicking the effects of the SYK inhibitor BAY61 in SH-SY5Y cells. Interestingly, LC3-I and LC3-II were both significantly decreased in the SYK knockdown cells, although their ratio remained unchanged (Fig. 6*A*). These data suggest that genetic suppression of SYK expression leads to an increased autophagy initiation (LC3-I conversion to LC3-II) and an enhancement of lysosomal LC3-II degra-

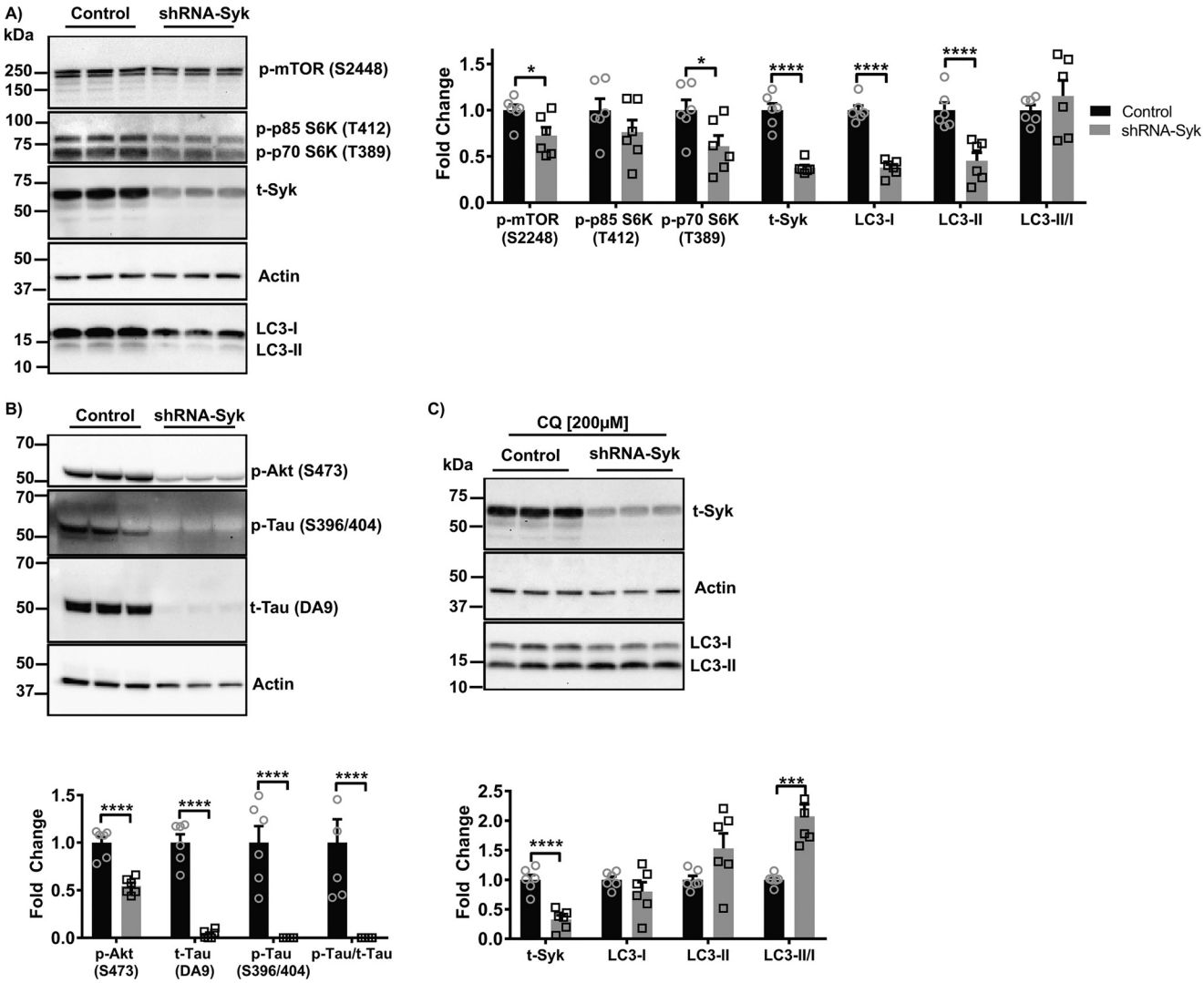

Figure 6. SYK knockdown mimics pharmacological inhibition of SYK and decreases total Tau levels. Lentiviral vectors expressing SYK-specific shRNAs or nonsense control shRNAs were used to stably knock down SYK gene expression in SH-SY5Y cells. *A* and *B*, representative Western blottings depicting p-mTOR (Ser-2448), p-S6K (Thr-389 and Thr-412), t-SYK, and LC3-I/II, as well as p-Akt (Ser-473), p-Tau (Ser-396/404), and t-Tau are shown. Western blot chemiluminescent signals were quantified by densitometry, normalized to actin, and presented as histograms. Unpaired *t* tests revealed that in SYK knockdown cells in which t-SYK was decreased significantly ($p < 0.0001$), p-mTOR (Ser-2448) ($p < 0.05$), p-S6K (Thr-389) ($p < 0.05$), p-Akt (Ser-473) ($p < 0.0001$), t-Tau ($p < 0.0001$), and p-Tau (Ser-396/404) ($p < 0.0001$) levels were also significantly decreased ($n = 6$). LC3-I and LC3-II levels were significantly decreased in SYK knockdown cells compared with control ($p < 0.0001$), but the ratio of both remains unchanged. *C*, both SYK knockdown and control cells were treated for 24 h with 200 μM of the lysosomal inhibitor CQ. Representative Western blottings depicting t-SYK and LC3-I/II are shown. Western blot chemiluminescent signals were quantified by densitometry, normalized to actin, and presented as histograms. Unpaired *t* tests revealed that in SYK knockdown cells in which t-SYK was decreased significantly ($p < 0.0001$), the ratio of LC3-II/I was significantly increased ($p < 0.001$) ($n = 6$ for each treatment condition).

dation. To further test this hypothesis, we treated both control and SYK knockdown cells for 24 h with 200 μM of the lysosomal inhibitor CQ. In the presence of CQ, the SYK knockdown cells exhibited a significantly increased ratio of LC3-II/I as observed in SH-SY5Y cells treated with CQ and BAY61, implying an increased autophagic flux and suggesting that SYK may impact both the autophagy initiation and lysosomal degradation (Fig. 6*C*).

Overall, our data show that the knockdown of SYK mimics the data obtained following pharmacological inhibition of SYK in SH-SY5Y cells resulting in an inhibition of key members of the mTOR pathway and further establishes a key role of SYK as an upstream modulator of the mTOR pathway (Fig. 7).

Chronic SYK inhibition reduces p-SYK and t-SYK levels in Tg Tau P301S mice, rescues neuronal and synaptic loss, and decreases mTOR activity

Following these *in vitro* studies, we investigated the effects of chronic SYK inhibition on Tau levels, neurodegeneration, inflammation, and behavior *in vivo* using a tauopathy mouse model. The 30-week-old Tg Tau P301S mice and age-matched wildtype (WT) littermates were treated for 12 weeks with 20 mg/kg of the SYK inhibitor BAY61 or PBS as a vehicle control (Fig. 8*A*). As we demonstrated previously (26), SYK activation, as measured by p-SYK (Tyr-525/526) levels, is significantly higher in Tg Tau P301S–PBS mice compared with WT controls (Fig. 8*B*). Importantly, the chronic treatment with the SYK

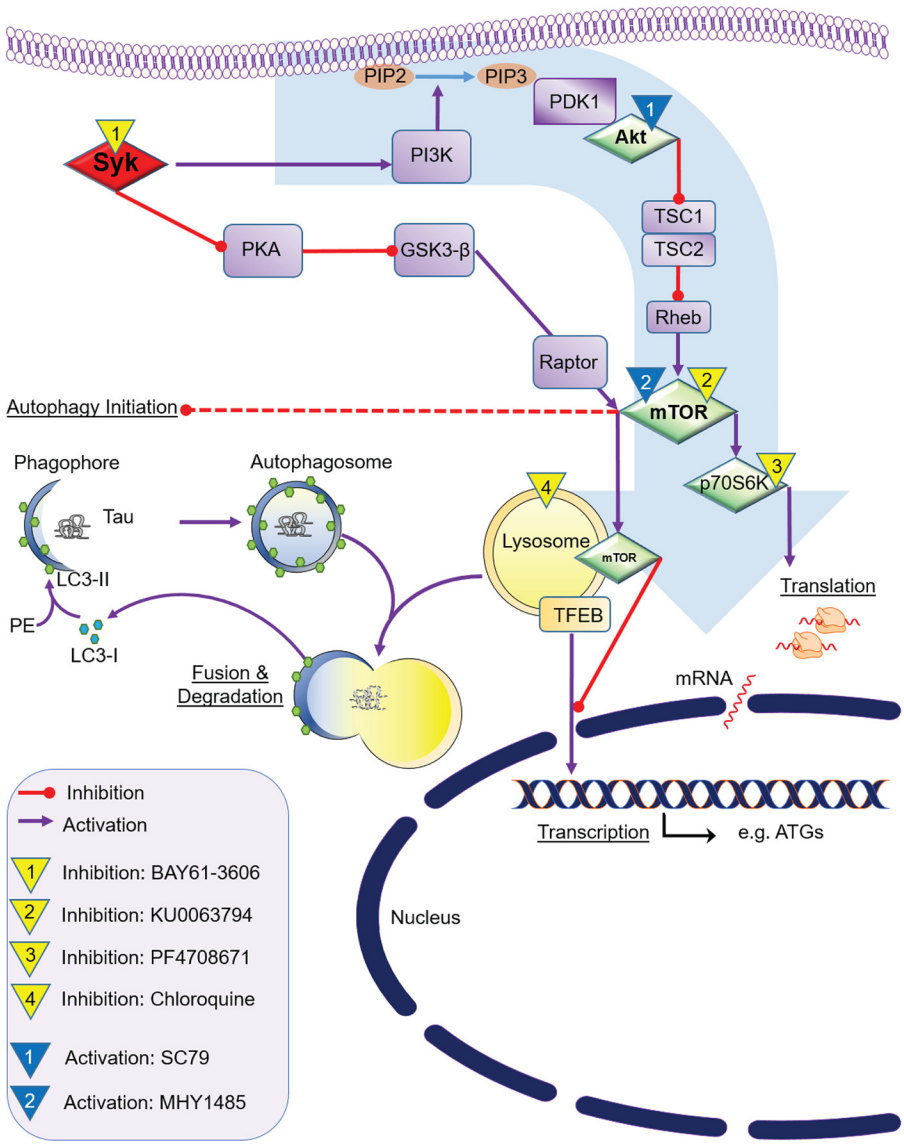

Figure 7. Schematic depiction of the role of SYK in the mTOR pathway and autophagy. The schematic describes the role of SYK in the mTOR pathway and autophagic tau degradation. The mTOR pathway, including PI3K, PDK1, Akt, TSC1/2, Rheb, mTOR, and S6K, and their role in regulation of autophagy have been well-described in the literature (for review see Ref. 82). Our previous studies revealed SYK as an upstream regulator of PKA, GSK-3β, and PI3K (25). PI3K is recognized as an upstream member of the mTOR pathway, and GSK3-β is known to regulate raptor, which is part of the mTOR complex I. In this study, we used different activators and inhibitors of members of the mTOR pathway (see legend) to elucidate the effect of SYK inhibition on the mTOR pathway. Our mechanistic experiments lead to the conclusion that SYK acts upstream of the mTOR pathway and thereby influences the activity levels of different members of that pathway and the autophagic degradation of Tau. mTOR itself is known to inhibit autophagy. mTOR prevents the transcription factor EB (*TFEB*) from entering the nucleus, thereby preventing the transcription of autophagy-related genes (ATGs), leading to a decreased autophagy initiation. Furthermore, the kinase S6K downstream of mTOR is involved in translation. Our results show that SYK inhibition leads to a decreased activation of the mTOR pathway and results in an increased autophagic flux (LC3-I to LC3-II conversion), leading to an increased lysosomal degradation of Tau.

inhibitor significantly reduced the elevated levels of p-SYK (Tyr-525/526) (Fig. 8*B*) confirming target engagement following treatment with BAY61. t-SYK levels were also increased in Tg Tau P301S–PBS mice compared with WT littermates and were significantly decreased following chronic SYK inhibition (Fig. 8*B*).

The neuron-specific protein NeuN (45) has been used previously as a marker for neurodegeneration or neuronal loss (46, 47). Neuronal loss revealed by a reduction in NeuN has been described previously in Tg Tau P301S mice (8, 12). Post-synaptic density-95 (PSD-95) has been shown to promote the stabilization of synapses and to regulate synaptic transmission (48–50). In addition, it has been established that levels of PSD-95 are significantly reduced in Tg Tau P301S mice and reflect synaptic loss (51, 52). We therefore investigated whether chronic inhibition of SYK with BAY61 was able to affect NeuN and PSD-95 levels in Tg Tau P301S mice. Our data show that PSD-95 and NeuN levels were reduced in Tg Tau P301S–PBS mice compared with WT littermates (Fig. 8) confirming previous observations (51, 52). Interestingly, the chronic treatment with the SYK inhibitor was able to considerably increase PSD-95 and NeuN levels in Tg Tau P301S mice (Fig. 8*B*), suggesting that SYK inhibition prevents neuronal and synaptic loss in Tg Tau P301S mice.

The p-mTOR (Ser-2448) levels were significantly increased in Tg Tau P301S–PBS mice compared with WT littermates

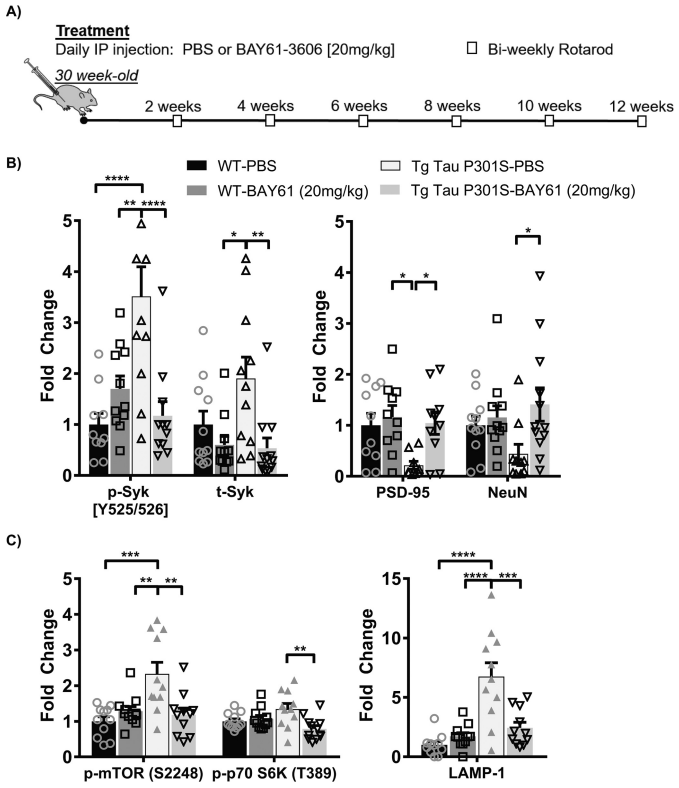

Figure 8. Chronic SYK inhibition reduces p-SYK and t-SYK levels in Tg Tau P301S mice, rescues neuronal and synaptic loss, and decreases mTOR activity. *A,* 30-week-old Tg Tau P301S mice and wildtype (*WT*) littermates were treated for 12 weeks with either PBS (control) or 20 mg/kg of the SYK inhibitor BAY61-3606 (administered i.p.) WT-PBS ($n = 11$), WT-BAY61 ($n = 11$), Tg Tau P301S–PBS ($n = 11$), and Tg Tau P301S–BAY61 ($n = 12$). Animals were tested for motor performance using the Rotarod every 14 days. *B* and *C,* PSD-95 levels were measured by ELISA. Levels of p-SYK, t-SYK, NeuN, p-mTOR (Ser-2448), p-S6K (Thr-389), and LAMP-1 were obtained by dot blots whose chemiluminescent signals were quantified and normalized to β-tubulin levels. All values are presented relative to WT-PBS (control). *B,* ANOVA with post hoc Bonferroni test revealed that SYK activation, as measured by p-SYK (Tyr-525/526) levels, was significantly increased in Tg Tau P301S–PBS mice compared with WT controls ($p < 0.0001$). Chronic treatment with 20 mg/kg of the SYK inhibitor BAY61-3606 reduced these levels significantly ($p < 0.0001$). t-SYK levels were also significantly reduced following treatment in Tg Tau P301S mice ($p < 0.01$). PSD-95 and NeuN levels were significantly increased ($p < 0.05$) following treatment with BAY61 in Tg Tau P301S mice compared with untreated (PBS) controls. *C,* ANOVA with post hoc Bonferroni test revealed that mTOR activation, as measured by p-mTOR (Ser-2448) levels, was significantly increased in Tg Tau P301S–PBS mice compared with WT controls ($p < 0.001$). Chronic treatment with 20 mg/kg of the SYK inhibitor BAY61-3606 reduced these levels significantly ($p < 0.01$). LAMP-1 levels were also significantly increased in Tg Tau P301S–PBS mice compared with WT controls ($p < 0.0001$). Chronic treatment with 20 mg/kg of the SYK inhibitor BAY61-3606 reduced these levels significantly ($p < 0.001$). The treatment also reduced p-S6K (Thr-389) levels significantly in Tg Tau P301S mice ($p < 0.01$).

(Fig. 8*C*), suggesting there might be an associated reduction in autophagy. As observed in our *in vitro* experiments, SYK inhibition was able to significantly decrease the abnormally high p-mTOR (Ser-2448) levels observed in Tg Tau P301S brains bringing them back to the levels observed in WT littermates (Fig. 8*C*). The p-S6K (Thr-389) levels were slightly elevated in Tg Tau P301S–PBS mice compared with WT littermates, and chronic SYK inhibition was able to significantly decrease p-S6K (Thr-389) levels in the brain of Tg Tau P301S mice (Fig. 8*C*), confirming an inhibition of the mTOR pathway. Interestingly, the lysosomal membrane–associated protein 1 (LAMP-1) was also significantly increased in Tg Tau P301S–PBS mice compared with WT littermates, whereas chronic SYK inhibition was able to significantly reduce LAMP-1 levels in the brains of Tg Tau P301S mice (Fig. 8*C*).

Chronic SYK inhibition reduces Tau accumulation and improves motor performance in Tg Tau P301S mice

Following the assessment of target engagement, we investigated the effects of chronic SYK inhibition on detergent-soluble and -insoluble Tau levels in the brains of Tg Tau P301S mice. We found that chronic SYK inhibition over a 12-week period significantly reduced the levels of t-Tau, p-Tau (Ser-396/404 and Ser-202), and Tau oligomers (TOC1) in the detergent-insoluble fraction of brain homogenates compared with PBS-treated Tg Tau P301S mice. A trend for a reduction in detergent insoluble p-Tau (Ser-231) and Tau conformers (MC1) was also observed following chronic SYK inhibition (Fig. 9*A*). Detergent-soluble total Tau levels were also reduced following SYK inhibition compared with PBS-treated Tg Tau P301S mice; however, only soluble p-Tau (Ser-231) was significantly impacted by SYK inhibition (Fig. 9*B*).

In addition to the reduced Tau burden, a significant improvement in locomotor coordination, measured by a decreased latency to fall in the rotarod apparatus, was observed in Tg Tau P301S mice following chronic inhibition of SYK (Fig. 9*C*).

Chronic SYK inhibition decreases neuroinflammation in Tg Tau P301S mice

Because SYK is known to be involved in the activation of microglia (21, 22), we investigated the effects of chronic SYK inhibition on neuroinflammation in Tg Tau P301S mice. As expected, the microglial marker Iba-1 was significantly increased in Tg Tau P301S–PBS mice compared with WT littermates (Fig. 10*A*). Chronic SYK inhibition was able to decrease Iba-1 levels significantly in Tg Tau P301S mice (Fig. 10*A*). We also investigated the levels of iNOS, which is known to be elevated in activated microglia (53). iNOS levels were found to be significantly increased in Tg Tau P301S–PBS mice compared with WT littermates (Fig. 10*A*). Chronic SYK inhibition appeared to significantly lower iNOS levels in Tg Tau P301S mice (Fig. 10*A*). Levels of the astrocytic marker, glial fibrillary acidic protein (GFAP), were similar with or without BAY61 treatment in WT and Tg Tau P301S mice (Fig. 10*A*). We also quantified by ELISA the amount of various pro-inflammatory cytokines in the brain. Overall, pro-inflammatory cytokine levels for most of the cytokines analyzed were higher in Tg Tau P301S–PBS mice compared with WT littermates and decreased in the Tg Tau P301S–BAY61 treatment group (Fig. 10*B*).

In summary, these data show that chronic SYK inhibition over a course of 12 weeks leads to significant reduction in neuronal and synaptic loss, inhibition of hyperactive mTOR, decreased Tau burden, improved motor performance, and suppression of neuroinflammation in Tg Tau P301S mice. Importantly, the decreased t-Tau and p-mTOR levels observed suggest that *in vivo* SYK inhibition also triggers the degradation of Tau via an autophagy-dependent mechanism similar to the one observed *in vitro*.

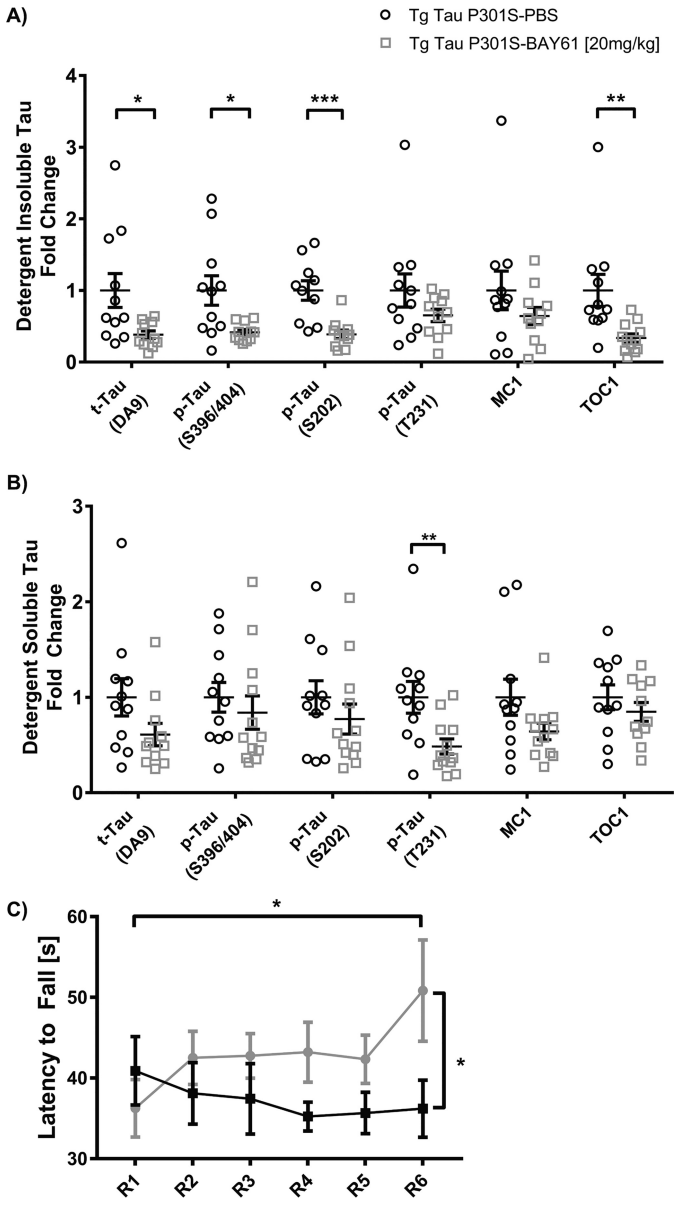

Figure 9. Chronic SYK inhibition reduces insoluble and soluble Tau levels and improves motor performance in Tg Tau P301S mice. 30-Week-old Tg Tau P301S mice and wildtype (WT) littermates were treated for 12 weeks with either PBS (control) or 20 mg/kg of the SYK inhibitor BAY61-3606 (administered i.p.) Tg Tau P301S–PBS ($n = 11$), Tg Tau P301S–BAY61 ($n = 12$). *A,* detergent (M-PER)-insoluble, and *B,* detergent (M-PER)-soluble Tau levels were obtained by dot blots whose chemiluminescent signals were quantified, normalized to β-tubulin levels, and expressed as a fold change of the average Tau values quantified in placebo-treated Tg Tau P301S mice. *A,* unpaired *t* tests revealed that insoluble total Tau levels ($p < 0.05$), as well as p-Tau (Ser-396/404 ($p < 0.05$) and Ser-202 ($p < 0.001$)) and Tau oligomers (TOC1) ($p < 0.01$) were significantly reduced following chronic SYK inhibition. *B,* soluble p-Tau (Ser-231) levels were reduced significantly following treatment with BAY61. *C,* animals' motor performance was tested using the rotarod every 14 days following the initiation of the BAY61 treatment. Two-way ANOVA with post hoc Bonferroni revealed a significant difference in motor performance for the last day (R6) between the control (Tg Tau P301S–PBS) mice and the mice treated with the SYK inhibitor. Motor performance of Tg Tau P301S–BAY61 mice improved significantly between the first and last day (*R1–R6*) of assessment but not in control.

Discussion

Our previous data have shown that SYK is up-regulated in the brain of AD patients and in mouse models of AD (26). In particular, we have shown that SYK is overactivated in neurons affected by the Tau pathology and that SYK up-regulation promotes Tau accumulation without affecting Tau expression (26). In this study, we show that SYK inhibition as well as genetic suppression of SYK expression lower total Tau levels in SH-SY5Y cells without impacting Tau expression at the mRNA level or Tau protein translation suggesting that other mechanisms are responsible for the increased Tau clearance observed following SYK inhibition. Therefore, we investigated the possible effects of SYK inhibition on the mTOR pathway and autophagic degradation of Tau in SH-SY5Y cells and in Tg Tau P301S following a chronic treatment with a SYK inhibitor as autophagy plays a pivotal role in Tau degradation (54).

We show for the first time that SYK can regulate the mTOR pathway in neuronal-like SH-SY5Y cells and promote the autophagic clearance of Tau. These data are consistent with previous studies that have highlighted the role of SYK on the mTOR pathway in immune and cancerous cells (55–61). Autophagy is crucial for maintaining the intracellular homeostasis by regulating the turnover of misfolded or damaged proteins and organelles and eliminating dysfunctional components. A decreased functionality of the autophagic degradation system has been linked to aging and neurodegenerative diseases (1–4, 62–66). Many studies have now demonstrated the beneficial effects of mTOR inhibition in mouse models of AD and tauopathy, resulting in increased autophagy and in an amelioration of Tau pathologies (11–13), suggesting that manipulating the mTOR pathway may constitute an attractive therapeutic strategy for the treatment of neurodegenerative proteinopathies.

In this study, we demonstrate that SYK inhibition leads to an increased total Tau degradation via the mTOR-dependent autophagy pathway, whereas transcription and translation levels of Tau remain unchanged. By examining the effects of SYK inhibition on members of the mTOR pathway, using selective inhibitors and activators of the mTOR pathway in combination with the SYK inhibitor BAY61, we confirmed that SYK acts upstream of the mTOR pathway and thereby modulates autophagy in a neuron-like cell line (SH-SY5Y). We show, for example, that the dysregulation of the mTOR pathway, as well as the Tau accumulation induced by the AKT stimulator SC79 or by MHY1485 (a direct activator of mTOR), can be reversed by SYK inhibition. We also confirm that inhibition of mTOR with KU0063794 can mimic the effects of SYK inhibition and increase the clearance of Tau in SH-SY5Y cells. In addition, the treatment with CQ in combination with the SYK inhibitor revealed an increased autophagic flux following SYK inhibition, as measured by an increase in the LC3II/I ratio, as well as mTOR and S6K inhibition and increased Tau degradation. To validate the data obtained with the SYK inhibitor BAY61, we also generated an SH-SY5Y cell line in which SYK has been stably knocked down. We confirm that Tau degradation is stimulated and that the mTOR pathway is also inhibited in this SYK knockdown cell line, showing that the effects of BAY61 on Tau clearance are recapitulated by genetic suppression of SYK expression and are therefore attributable to an inhibition of SYK.

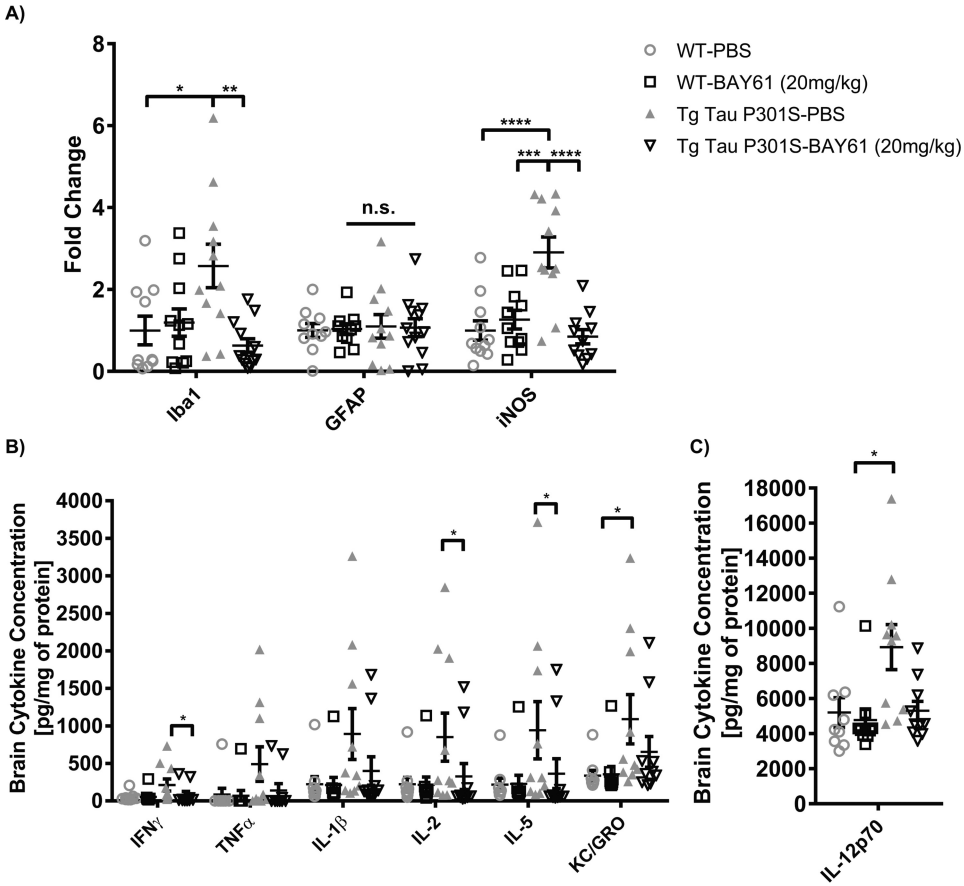

Figure 10. Chronic SYK inhibition decreases microgliosis and reduces pro-inflammatory cytokines in Tg Tau P301S mice. 30-Week-old Tg Tau P301S mice and wildtype (*WT*) littermates were treated for 12 weeks with either PBS (control) or 20 mg/kg of the SYK inhibitor BAY61-3606 (administered i.p.) WT-PBS ($n = 11$), WT-BAY61 ($n = 11$), Tg Tau P301S–PBS ($n = 11$), and Tg Tau P301S–BAY61 ($n = 12$). *A*, Iba-1, GFAP, and iNOS levels were obtained by dot blots whose chemiluminescent signals were quantified, normalized to β-tubulin levels, and expressed as a fold change of the average tau values quantified in placebo-treated Tg Tau P301S mice. ANOVA with Bonferroni tests revealed that Iba-1 ($p < 0.05$) and iNOS ($p < 0.0001$) levels were significantly increased in Tg Tau P301S–PBS mice compared with WT-PBS mice suggesting that microglia are activated in Tg Tau P301S mice. Chronic SYK inhibition significantly reduced Iba-1 ($p < 0.01$) and iNOS ($p < 0.0001$) levels in Tg Tau P301S mice. GFAP levels did not differ significantly between the groups. *B* and *C*, brain cytokine levels were quantified by ELISA and normalized to total protein levels. *B* and *C*, Kruskal-Wallis test revealed that the elevated brain cytokine levels observed in Tg Tau P301S–PBS (control) mice were significantly reduced following chronic SYK inhibition (Tg Tau P301S–BAY61) for interferon-γ ($p < 0.05$), IL-2 ($p < 0.05$), IL-5 ($p < 0.05$), and IL12p70; KC/GRO levels were significantly increased ($p < 0.05$) in Tg Tau P301S–PBS mice compared with WT controls.

We then assessed the impact of a chronic SYK inhibition with BAY61 in a pure model of tauopathy, Tg Tau P301S mice. SYK inhibition was initiated in 30-week-old Tg Tau P301S mice. By that age, Tg Tau P301S mice already show significant Tau accumulation and hyperphosphorylation as well as neuroinflammation and synaptic loss (51). We treated Tg Tau P301S mice for 12 weeks with BAY61 and observed that the treatment was well-tolerated and was not affecting the weight of the mice or the weight of major organs (data not shown). Behavioral analyses revealed that locomotor performances of the Tg Tau P301S mice were improved following SYK inhibition in the rotarod apparatus. Our biochemical characterizations of the brains of these mice confirmed our previous findings that SYK activation is increased in Tg Tau P301S mice (26), and they reveal target engagement following BAY61 treatment, as the autophosphorylation of SYK in the activation loop of the kinase was significantly reduced in Tg Tau P301S mice treated with BAY61. We found that mTOR activation was increased in Tg Tau P301S mice compared with WT littermates, suggesting that autophagy could be decreased and contribute to pathological Tau accumulation in Tg Tau P301S mice. Tg Tau P301S mice treated with the SYK inhibitor showed a reduction of mTOR activation confirming the *in vitro* data showing the impact of SYK on the regulation of the mTOR pathway.

We analyzed the impact of SYK inhibition on the accumulation of Tau pathogenic species in the soluble and insoluble detergent fractions of Tg Tau P301S brain homogenates. Detergent-insoluble Tau species have been shown to generally contain Tau aggregates that contribute to neurodegeneration (66, 67), whereas hyperphosphorylated Tau in the detergent-soluble fraction has previously been associated with synaptic loss (68). We found that t-Tau levels, as well as p-Tau (Ser-396/404 and Ser-202) levels and Tau oligomers (TOC1), were significantly decreased in the detergent-insoluble fraction, following SYK inhibition in Tg Tau P301S mice. Given that mTOR phosphorylation was reduced following SYK inhibition in Tg Tau P301S mice, these data further suggest that the decreased accumulation of the pathological Tau species observed results in part from an increased Tau degradation via the restored mTOR–autophagy pathway.

It is well-known that tauopathies, including AD and frontotemporal dementia with parkinsonism-17 (FTDP-17), lead to

neurodegeneration. In mouse models of tauopathy, including the Tg Tau P301S mice, reduced levels of the neuronal marker NeuN have been found and interpreted as evidence of neurodegeneration (12, 13). Interestingly, it has been shown (13) that NeuN levels were restored in Tg Tau P301S mice following stimulation of autophagy. In addition, it was found that stimulation of autophagy in Tg Tau P301S mice can decrease insoluble Tau, as well as p-Tau (AT100 and PHF-1) levels (12, 13). The results of our study are in line with these findings. We also observed decreased levels of synaptic and neuronal markers PSD-95 and NeuN in Tg Tau P301S mice, which were considerably increased following chronic SYK inhibition, suggesting that SYK inhibition can prevent neurodegeneration and synaptic loss induced by Tau pathogenic species in Tg Tau P301S mice.

Neuroinflammation has been shown previously to be increased in Tg Tau P301S mice (51, 69) and is likely to exacerbate the neurodegeneration and Tau pathology (69). We carefully investigated the impact of chronic SYK inhibition on neuroinflammation in Tg Tau P301S mice by analyzing the levels of various pro-inflammatory cytokines and by quantifying Iba-1 and iNOS levels as markers of microgliosis (70, 71), as well as GFAP to measure astrogliosis (72). We found that Iba-1, iNOS, and various pro-inflammatory cytokine levels were markedly increased in Tg Tau P301S mice compared with WT littermates, whereas GFAP levels were unchanged. Chronic SYK inhibition appeared to significantly reduce Iba-1, iNOS, and pro-inflammatory cytokine levels in Tg Tau P301S mice suggesting that SYK plays a key role in the induction of neuroinflammation by Tau pathogenic species. Pro-inflammatory cytokines produced by activated microglia have been shown to promote Tau hyperphosphorylation (73, 74), and therefore, SYK inhibition by directly targeting the activation of microglia could also contribute to the decreased Tau hyperphosphorylation observed.

Several studies have linked neuroinflammation and a deficit of autophagy in the context of neurodegenerative diseases. It has been shown, for example, that mTOR or S6K inhibition by rapamycin or PF4708671, respectively, prevents neuroinflammation in a mouse model of cerebral palsy (75). In that mouse model, the mice were subjected to hypoxia–ischemia and LPS-induced inflammation on day 6 after birth. Zheng *et al.* (76) showed that 5 mg/kg LPS injected intraperitoneally into C57BL/6J mice at 3 and 16 months of age not only leads to increased neuroinflammation but also to an autophagic impairment. Zhou *et al.* (77) demonstrated that GSK-3β inhibition suppressed neuroinflammation in the cortices of rats subjected to ischemic brain injury by activating autophagy. In another study, it was observed that neuroinflammation can block the autophagic flux in rats subjected to stress-induced hypertension (67). It has also been suggested that glial cells play a major role in the development of autophagy deficits observed in HIV-associated dementia (78). In conclusion, these studies suggest that a pathological disruption of autophagy can cause an initiation or exacerbation of neuroinflammation, and conversely, neuroinflammation can induce an autophagic deficit further contributing to neurodegeneration. Our data show that SYK is involved in both the regulation of autophagy as well as neuroinflammation and suggest that SYK may represent an important therapeutic target for the treatment of neurodegenerative proteinopathies. We found increased LAMP-1 levels in Tg Tau P301S compared with WT littermates, which could be indicative of a lysosomal defect in Tg Tau P301S. Interestingly, LAMP-1 levels were reduced in Tg Tau P301S mice following SYK inhibition, which could suggest that lysosomal functions were also improved by the treatment. Bain *et al.* (79) found that in some cases the pathological mechanism in FTLD–Tau may be attributed to lysosomal deficiencies and impaired transport, as LAMP-1 levels were increased suggesting the presence of more lysosomes. They concluded that FTLD cases with an underlying granulin mutation show TAR DNA-binding protein (TDP-43) aggregates because of a lysosomal dysfunction (impaired degradation) rather than a lysosomal deficiency (lack of lysosomes). In our study, we show that Tg Tau P301S mice exhibit elevated levels of LAMP-1, along with increased Tau levels compared with WT littermates. Because LAMP-1 levels are increased and suggest higher numbers of lysosomes or increased lysosomal surface area, a lysosomal defect or a dysfunctional transport, as suggested by Bain *et al.* (79), could also contribute to the accumulation of Tau in Tg Tau P301S mice. It is possible that the increased LAMP-1 levels observed in Tg Tau P301S mice represent a compensatory mechanism, initiated to counteract the lysosomal dysfunction. Interestingly, the treatment with the SYK inhibitor decreased Tau, as well as LAMP-1 levels significantly, suggesting an improvement of lysosomal functions. The analysis of the ratio of LC3-II/I in stable SYK knockdown cells alone and in the presence of the lysosome inhibitor CQ also indicate a possible role of SYK in lysosomal degradation. The role of SYK in lysosomal functions will need to be further delineated in future experiments.

The data presented in this study illustrate the dual role of SYK as a regulator of neuroinflammation and autophagy in the central nervous system. The observations made in this study not only provide further evidence for an important role of SYK in the pathogenesis of AD and the development of Tau pathologies but also demonstrate that pharmacological SYK inhibition may represent a promising therapeutic strategy for the treatment of AD and other neurodegenerative proteinopathies.

Experimental procedures

Animals

All mice were maintained under specific pathogen-free conditions in ventilated racks in the Association for Assessment and Accreditation of Laboratory Animal Care International (AAALAC) accredited vivarium of the Roskamp Institute. All experiments involving mice were reviewed and approved by the Institutional Animal Care and Use Committee of the Roskamp Institute before implementation and were conducted in compliance with the National Institutes of Health Guidelines for the Care and Use of Laboratory Animals. Tg Tau P301S (51) mice were obtained from The Jackson Laboratory and were bred with C57BL/6J mice to produce the Tg Tau P301S and WT littermates used in this study.

In vivo treatment

The 30-week-old Tg Tau P301S mice and wildtype (WT) littermates were injected with either PBS (vehicle) or 20 mg/kg of the SYK inhibitor BAY61 5 consecutive days per week for a total of 12 weeks. 45 animals were treated in total (WT-PBS ($n = 11$), WT-BAY61 ($n = 11$), Tg Tau P301S–PBS ($n = 11$), and Tg Tau P301S–BAY61 ($n = 12$)). The 2-(7-(3,4-dimethoxyphenyl)imidazo[1,2-*c*]pyrimidin-5-ylamino) nicotinamide hydrochloride hydrate (BAY61-3606) was synthesized as described previously (80). The identity and purity of the compound obtained were analyzed by tandem mass spectroscopy (MS (ESI, positive ion) *m/z* 391.1 (M + 1)). The activity of the synthesized BAY61 was further compared against a batch of BAY61 obtained by a commercial vendor (Sigma) by assessing its potency for inhibiting p65NFκB and STAT3 phosphorylation induced by TNFα in SH-SY5Y cells as described previously (data not shown) (25).

Behavioral analysis

Motor performance was assessed using a Rotarod apparatus every 14 days. The mice were placed onto a horizontally-oriented rotating cylinder. The baseline level was set to 5 rpm. The speed of the rotation of the cylinder was set up to increase to 50 rpm within 1 min. The latency to fall was measured in seconds. Each mouse underwent three trials per day, and the average latency to fall was calculated. Mice showing signs of partial paralysis of the hind limbs were excluded from the behavioral assessments.

Tissue processing

All mice were humanely euthanized, and their brains were collected. The right hemisphere was snap-frozen in liquid nitrogen and stored at −80 °C until processing. The method of euthanasia used follows the American Veterinary Medical Association (AVMA) guidelines for the euthanasia of animals. Briefly, mice were rendered unconscious through inhalation of 5% isoflurane in oxygen using a vaporizer and a gas chamber. While under anesthesia, after verifying the absence of reflexes, mice were euthanatized by exsanguination (blood was withdrawn from cardiac puncture).

The right hemispheres were homogenized in Mammalian Protein Extraction Reagent (M-PER™, Thermo Fisher Scientific) containing Halt protease and phosphatase single use inhibitor/EDTA (Thermo Fisher Scientific) and 1 mM PMSF. Brain homogenates were centrifuged at 4 °C, 21,817 × *g* for 30 min. The supernatant (detergent-soluble fraction) was collected and stored at −80 °C until being assayed for total Tau and phosphorylated Tau as described below. The pellet (detergent-insoluble fraction) was resuspended by sonication in M-PER (1:1 v/v). A portion of this detergent-insoluble fraction was treated with an equal volume of 5 M guanidine isothiocyanate to dissociate and re-solubilize Tau aggregates and to quantify the amount of detergent-insoluble total Tau and phosphorylated Tau at multiple epitopes as described below. The remaining portion of the detergent-insoluble fraction was used to assess the levels of Tau oligomers and Tau pathogenic conformers under native conditions as described below.

Cell culture

SH-SY5Y cells were purchased from American Type Culture Collection (Manassas, VA). SH-SY5Y cells were grown in Dulbecco's modified Eagle's medium/F-12 medium (Thermo Fisher Scientific) supplemented with 10% fetal bovine serum (Thermo Fisher Scientific), GlutaMAX, and 1% penicillin/streptomycin/fungizone.

Cell culture treatments

SH-SY5Y cells were treated in 500 μl of medium for 24 h using 24-well cell culture plates. The cells were treated with the following inhibitors/activators: SYK inhibitor BAY61 (5–10 μM, Sigma), Akt activator SC79 (20 μM, Sigma), mTOR activator MHY1485 (4–12 μM, Sigma), mTOR inhibitor KU0063794 (1–2 μM, Sigma), S6K inhibitor PF4708671 (5–10 μM, Tocris), and lysosomal inhibitor CQ (100–200 μM, Tocris).

SH-SY5Y differentiation

SH-SY5Y cells were differentiated as described previously by Encinas *et al.* (28). Briefly, SH-SY5Y cells were seeded into 24-well plates and treated with 10 μM retinoic acid in media containing 15% fetal bovine serum for 5 days. Subsequently, the cells were treated with 50 ng/ml BDNF for 7 days in media containing no serum.

Puromycin incorporation assay

To investigate the possible impact of SYK inhibition on protein synthesis, we used the SUnSET technique (43). This technique involves the use of the antibiotic puromycin (a structural analog of tyrosyl-tRNA), and anti-puromycin antibodies to detect the amount of puromycin incorporation into nascent peptide chains. Incorporation of puromycin into nascent polypeptides causes termination. Although a high concentration of puromycin is toxic because it can inactivate translation, at low concentrations it provides an accurate snapshot of protein synthesis without causing lethality. Confluent SH-SY5Y cells were treated with BAY61 and PF4708671 for 24 h and with cycloheximide for 5 h. Cells were then treated for 1 h with 10 μg/ml puromycin and lysed in ice-cold M-PER (Thermo Fisher Scientific) containing Halt protease and phosphatase single use inhibitor/EDTA (Thermo Fisher Scientific) and 1 mM PMSF. Levels of newly synthesized proteins containing puromycin were then detected by Western blotting using an anti-puromycin antibody (1:1000 dilution, Millipore Sigma).

Immunoprecipitation (IP)

Following the SUnSET technique, cell lysates were centrifuged at 16,000 × *g* for 15 min at 4 °C to remove the insoluble fractions. The resulting supernatants were subjected to IP with 2 μg/ml anti-puromycin (Millipore Sigma) overnight at 4 °C. Then, 20 μl of protein A-magnetic beads (Thermo Fisher Scientific) were added for 2 h at 4 °C. The beads were carefully washed, and the proteins were eluted with reducing 2× Laemmli sample buffer (Bio-Rad) at 95 °C for 5 min. The samples were then analyzed by Western blotting.

Quantitative RT-PCR

Total RNA was extracted from SH-SY5Y cells treated with DMSO or BAY61 using the TRIzol reagent (Invitrogen). RNA

was reverse-transcribed into first-strand cDNA using the SuperScript™ III first-strand synthesis system (Invitrogen). Quantitative real-time PCR (qPCR) was performed with ssoAdvanced™ Universal SYBR® Green Supermix (Bio-Rad) and analyzed on a CFX96 Touch™ Real-Time PCR Detection System (Bio-Rad) as per the manufacturer's instructions. The mRNA levels in each sample were analyzed by normalizing the threshold cycle (*Ct*) value to that of internal loading control, β-actin, employing the primer sets used for human total and 3R Tau detection that have been described previously (81).

Generation of SYK knockdown SH-SY5Y cells

Short hairpin RNAs (shRNAs) were used to stably knock down SYK gene expression in SH-SY5Y cells. GIPZ lentiviral vectors expressing SYK-specific shRNAs (25) or nonsense control shRNAs were purchased from Origene. For stable transfection, SH-SY5Y cells were grown on 6-well plates until reaching 70–80% confluence and transfected with shRNA plasmids using Lipofectamine 2000 (Invitrogen). After 48 h, transfected cells were placed into fresh medium in the presence of 1 μg/ml puromycin for selection. After 14 days, the resistant cells were trypsinized and expanded. The knockdown efficiency of SYK was confirmed by Western blotting using antibodies against SYK (4D10, Santa Cruz Biotechnology).

Immunoblotting

Western blots were performed as described previously (25, 26). Briefly, SH-SY5Y cells were cultured in 24-well plates, treated for 24 h, and subsequently lysed with mammalian protein extraction reagent (MPER, Thermo Fisher Scientific) containing Halt protease and phosphatase single use inhibitor/EDTA (Thermo Fisher Scientific) and 1 mM PMSF. Proteins of cell lysates were separated by 10% Tris-glycine–SDS-PAGE using 1-mm Criterion TGX gels (Bio-Rad) and electrotransferred onto 0.2-μm polyvinylidene difluoride membranes (Bio-Rad). For dot blots, 3 μl of each sample were pipetted onto a nitrocellulose membrane (pore size 45 μm, Bio-Rad). Membranes were blocked in TBS containing 5% nonfat dried milk for 1 h and were hybridized with the primary antibodies (anti-SYK (4D10), 1:1000, Santa Cruz Biotechnology), anti-p-Tau Ser-396/404 (PHF-1, 1:1000, Dr. Peter Davies' lab), anti-t-Tau (DA9, 1:1000, Dr. Peter Davies' lab), anti-p-Tau Ser-202 (CP13, 1:1000, Dr. Peter Davies' lab), anti-p-Tau Thr-231 (RZ3, 1:1000, Dr. Peter Davies' lab), anti-conformer-Tau (MC1, 1:1000, Dr. Peter Davies' lab), anti-oligomeric-Tau (TOC1, 1:1000, Dr. Lester Binder's lab) anti-p-SYK (Tyr-525/526), anti-p-mTOR (Ser-2448), anti-p-S6K (Thr-389/Thr-412), anti-p-Akt (Ser-473), anti-LC3b, anti-actin, anti-NeuN, anti-LAMP-1, anti-iNOS (all 1:1000, Cell Signaling), anti-GFAP (1:5000, DAKO), anti-Iba1 (1:1000, Abcam, MA), and anti-β-tubulin (1:1000, BD Biosciences) overnight at 4 °C. Subsequently, the membranes were incubated for 1 h in horseradish peroxidase–conjugated anti-mouse or anti-rabbit secondary antibody (1:1000, Cell Signaling). Western blottings and dot blots were visualized using chemiluminescence (Super Signal West Femto Maximum Sensitivity Substrate, Thermo Fisher Scientific). Signals were quantified using ChemiDoc XRS (Bio-Rad), and densitometric analyses were performed using Quantity One (Bio-Rad) image analysis software.

Total protein concentration (BCA)

Total protein levels of *in vivo* samples were determined using the Pierce BCA protein assay kit (Thermo Fisher Scientific). The samples were prepared and measured as directed by the manufacturer's handbook.

ELISA for PSD-95 and cytokine levels

For quantification of *in vivo* PSD-95 and cytokine levels, the MESO QuickPlex SQ 120 and the appropriate ELISA kits were used (Meso Scale Diagnostics). The samples were prepared and measured as directed by the manufacturer's instructions. Then 16 wells were used for the standard. 10 samples (brain homogenates) from each treatment group were randomly selected. The values for all brain samples were normalized to total protein level as determined by the BCA method.

Statistical analyses

The data were analyzed and plotted with GraphPad Prism (GraphPad Software, Inc.). The Shapiro-Wilk test for normality was used to test for Gaussian distribution. Statistical significance was determined by either ANOVA (for comparisons of three or more groups), two-way ANOVA (behavioral test), or *t* tests (SYK knockdown) or the nonparametric Kruskal-Wallis (Cytokine ELISA), where appropriate for data that were not normally distributed. The ROUT test ($Q = 1\%$) was used for the identification or rejection of statistical outliers. All data are presented as mean ± S.E., and $p < 0.05$ was considered significant (*, $p < 0.05$; **, $p < 0.01$; ***, $p < 0.001$; ****, $p < 0.0001$).

Author contributions—J. E. S., F. C., M. M., and D. P. conceptualization; J. E. S., H. Y., K. C., and D. P. data curation; J. E. S., H. Y., and D. P. formal analysis; J. E. S., H. Y., K. C., C. J., and D. P. investigation; J. E. S. visualization; J. E. S., H. Y., C. J., and D. P. methodology; J. E. S. writing-original draft; J. E. S., M. M., and D. P. writing-review and editing; C. J. resources; F. C., M. M., and D. P. supervision; F. C. and D. P. funding acquisition; F. C., M. M., and D. P. project administration; D. P. validation.

Acknowledgments—We are grateful to Dr. Peter Davies (Litwin-Zucker Center for Research on Alzheimer's Disease, Feinstein Institute, Manhasset, NY) for kindly providing the PHF-1, CP13, MC1, RZ3, and DA9 antibodies. We thank the late Dr. Lester Binder (Feinberg School of Medicine, Northwestern University, Chicago, IL) for providing the TOC1 antibody.

References

1. Nixon, R. A. (2007) Autophagy, amyloidogenesis and Alzheimer disease. *J. Cell Sci.* **120,** 4081–4091 CrossRef Medline
2. Nixon, R. A., and Yang, D.-S. (2011) Autophagy failure in Alzheimer's disease–locating the primary defect. *Neurobiol. Dis.* **43,** 38–45 CrossRef Medline
3. Ghavami, S., Shojaei, S., Yeganeh, B., Ande, S. R., Jangamreddy, J. R., Mehrpour, M., Christoffersson, J., Chaabane, W., Moghadam, A. R., Kashani, H. H., Hashemi, M., Owji, A. A., and Łos, M. J. (2014) Autophagy and apoptosis dysfunction in neurodegenerative disorders. *Prog. Neurobiol.* **112,** 24–49 CrossRef Medline

4. Menzies, F. M., Fleming, A., and Rubinsztein, D. C. (2015) Compromised autophagy and neurodegenerative diseases. *Nat. Rev. Neurosci.* **16,** 345–357 CrossRef Medline
5. Jung, C. H., Ro, S.-H., Cao, J., Otto, N. M., and Kim, D.-H. (2010) mTOR regulation of autophagy. *FEBS Lett.* **584,** 1287–1295 CrossRef Medline
6. Zare-Shahabadi, A., Masliah, E., Johnson, G. V., and Rezaei, N. (2015) Autophagy in Alzheimer's disease. *Rev. Neurosci.* **26,** 385–395 CrossRef Medline
7. Kragh, C. L., Ubhi, K., Wyss-Corey, T., and Masliah, E. (2012) Autophagy in dementias. *Brain Pathol.* **22,** 99–109 CrossRef Medline
8. Wang, I.-F., Guo, B.-S., Liu, Y.-C., Wu, C.-C., Yang, C.-H., Tsai, K.-J., and Shen, C.-K. (2012) Autophagy activators rescue and alleviate pathogenesis of a mouse model with proteinopathies of the TAR DNA-binding protein 43. *Proc. Natl. Acad. Sci. U.S.A.* **109,** 15024–15029 CrossRef Medline
9. Puertollano, R. (2014) mTOR and lysosome regulation. *F1000Prime Rep.* **6,** 52 CrossRef Medline
10. Ozcelik, S., Fraser, G., Castets, P., Schaeffer, V., Skachokova, Z., Breu, K., Clavaguera, F., Sinnreich, M., Kappos, L., Goedert, M., Tolnay, M., and Winkler, D. T. (2013) Rapamycin attenuates the progression of tau pathology in P301S tau transgenic mice. *PLoS One* **8,** e62459 CrossRef Medline
11. Jiang, T., Yu, J.-T., Zhu, X.-C., Zhang, Q.-Q., Cao, L., Wang, H.-F., Tan, M.-S., Gao, Q., Qin, H., Zhang, Y.-D., and Tan, L. (2014) Temsirolimus attenuates tauopathy *in vitro* and *in vivo* by targeting tau hyperphosphorylation and autophagic clearance. *Neuropharmacology* **85,** 121–130 CrossRef Medline
12. Schaeffer, V., Lavenir, I., Ozcelik, S., Tolnay, M., Winkler, D. T., and Goedert, M. (2012) Stimulation of autophagy reduces neurodegeneration in a mouse model of human tauopathy. *Brain* **135,** 2169–2177 CrossRef Medline
13. Wang, H., Wang, R., Carrera, I., Xu, S., and Lakshmana, M. K. (2016) TFEB overexpression in the P301S model of tauopathy mitigates increased PHF1 levels and lipofuscin puncta and rescues memory deficits. *eNeuro* **3,** ENEURO.0042-16.2016 CrossRef Medline
14. Elías, E. E., Almejún, M. B., Colado, A., Cordini, G., Vergara-Rubio, M., Podaza, E., Risnik, D., Cabrejo, M., Fernández-Grecco, H., Bezares, R. F., Custidiano, M. D. R., Sánchez-Ávalos, J. C., Vicente, Á., Garate, G. M., Borge, M., *et al.* (2018) Autologous T cell activation fosters ABT-199 resistance in chronic lymphocytic leukemia: rationale for a combined therapy with SYK inhibitors and anti-CD20 MoAbs. *Haematologica* **103,** e458–e461 CrossRef Medline
15. Hayashi, H., Kaneko, R., Demizu, S., Akasaka, D., Tayama, M., Harada, T., Irie, H., Ogino, Y., Fujino, N., and Sasaki, E. (2018) TAS05567, a novel potent and selective spleen tyrosine kinase inhibitor, abrogates immunoglobulin-mediated autoimmune and allergic reactions in rodent models. *J. Pharmacol. Exp. Ther.* **366,** 84–95 CrossRef Medline
16. Park, J.-E., Majumdar, S., Brand, D. D., Rosloniec, E. F., Yi, A.-K., Stuart, J. M., Kang, A. H., and Myers, L. K. (2018) The role of Syk in peripheral T cells. *Clin. Immunol.* **192,** 50–57 CrossRef Medline
17. Roders, N., Herr, F., Ambroise, G., Thaunat, O., Portier, A., Vazquez, A., and Durrbach, A. (2018) SYK inhibition induces apoptosis in germinal center-like B cells by modulating the antiapoptotic protein myeloid cell leukemia-1, affecting B-cell activation and antibody production. *Front. Immunol.* **9,** 787 CrossRef Medline
18. Faruki, S., Geahlen, R. L., and Asai, D. J. (2000) Syk-dependent phosphorylation of microtubules in activated B-lymphocytes. *J. Cell Sci.* **113,** 2557–2565 Medline
19. Tsujimura, T., Yanagi, S., Inatome, R., Takano, T., Ishihara, I., Mitsui, N., Takahashi, S., and Yamamura, H. (2001) Syk protein-tyrosine kinase is involved in neuron-like differentiation of embryonal carcinoma P19 cells. *FEBS Lett.* **489,** 129–133 CrossRef Medline
20. Yu, Y., Gaillard, S., Phillip, J. M., Huang, T.-C., Pinto, S. M., Tessarollo, N. G., Zhang, Z., Pandey, A., Wirtz, D., Ayhan, A., Davidson, B., Wang, T.-L., and Shih, I.-M. (2015) Inhibition of spleen tyrosine kinase potentiates paclitaxel-induced cytotoxicity in ovarian cancer cells by stabilizing microtubules. *Cancer Cell* **28,** 82–96 CrossRef Medline
21. Combs, C. K., Johnson, D. E., Cannady, S. B., Lehman, T. M., and Landreth, G. E. (1999) Identification of microglial signal transduction pathways mediating a neurotoxic response to amyloidogenic fragments of β-amyloid and prion proteins. *J. Neurosci.* **19,** 928–939 CrossRef Medline
22. McDonald, D. R., Brunden, K. R., and Landreth, G. E. (1997) Amyloid fibrils activate tyrosine kinase-dependent signaling and superoxide production in microglia. *J. Neurosci.* **17,** 2284–2294 CrossRef Medline
23. Combs, C. K., Karlo, J. C., Kao, S. C., and Landreth, G. E. (2001) β-Amyloid stimulation of microglia and monocytes results in TNFα-dependent expression of inducible nitric oxide synthase and neuronal apoptosis. *J. Neurosci.* **21,** 1179–1188 CrossRef Medline
24. Ghosh, S., and Geahlen, R. L. (2015) Stress granules modulate SYK to cause microglial cell dysfunction in Alzheimer's disease. *EBioMedicine* **2,** 1785–1798 CrossRef Medline
25. Paris, D., Ait-Ghezala, G., Bachmeier, C., Laco, G., Beaulieu-Abdelahad, D., Lin, Y., Jin, C., Crawford, F., and Mullan, M. (2014) The spleen tyrosine kinase (Syk) regulates Alzheimer amyloid-β production and Tau hyperphosphorylation. *J. Biol. Chem.* **289,** 33927–33944 CrossRef Medline
26. Schweig, J. E., Yao, H., Beaulieu-Abdelahad, D., Ait-Ghezala, G., Mouzon, B., Crawford, F., Mullan, M., and Paris, D. (2017) Alzheimer's disease pathological lesions activate the spleen tyrosine kinase. *Acta Neuropathol. Commun.* **5,** 69 CrossRef Medline
27. Yamamoto, N., Takeshita, K., Shichijo, M., Kokubo, T., Sato, M., Nakashima, K., Ishimori, M., Nagai, H., Li, Y.-F., Yura, T., and Bacon, K. B. (2003) The orally available spleen tyrosine kinase inhibitor 2–7-(3,4-dimethoxyphenyl)-imidazo1,2-cpyrimidin-5-ylaminonicotinamide dihydrochloride (BAY 61-3606) blocks antigen-induced airway inflammation in rodents. *J. Pharmacol. Exp. Ther.* **306,** 1174–1181 CrossRef Medline
28. Encinas, M., Iglesias, M., Liu, Y., Wang, H., Muhaisen, A., Ceña, V., Gallego, C., and Comella, J. X. (2000) Sequential treatment of SH-SY5Y cells with retinoic acid and brain-derived neurotrophic factor gives rise to fully differentiated, neurotrophic factor-dependent, human neuron-like cells. *J. Neurochem.* **75,** 991–1003 CrossRef Medline
29. Wang, X., and Proud, C. G. (2011) mTORC1 signaling: what we still don't know. *J. Mol. Cell Biol.* **3,** 206–220 CrossRef Medline
30. Choi, Y. J., Park, Y. J., Park, J. Y., Jeong, H. O., Kim, D. H., Ha, Y. M., Kim, J. M., Song, Y. M., Heo, H.-S., Yu, B. P., Chun, P., Moon, H. R., and Chung, H. Y. (2012) Inhibitory effect of mTOR activator MHY1485 on autophagy: suppression of lysosomal fusion. *PLoS One* **7,** e43418 CrossRef Medline
31. Chuang, J.-Y., Huang, Y.-L., Yen, W.-L., Chiang, I.-P., Tsai, M.-H., and Tang, C.-H. (2014) Syk/JNK/AP-1 signaling pathway mediates interleukin-6-promoted cell migration in oral squamous cell carcinoma. *Int. J. Mol. Sci.* **15,** 545–559 CrossRef Medline
32. Lee, C. K., Yang, Y., Chen, C., and Liu, J. (2016) Syk-mediated tyrosine phosphorylation of mule promotes TNF-induced JNK activation and cell death. *Oncogene* **35,** 1988–1995 CrossRef Medline
33. Zhang, J., Gao, Z., and Ye, J. (2013) Phosphorylation and degradation of S6K1 (p70S6K1) in response to persistent JNK1 activation. *Biochim. Biophys. Acta* **1832,** 1980–1988 CrossRef Medline
34. García-Martínez, J. M., Moran, J., Clarke, R. G., Gray, A., Cosulich, S. C., Chresta, C. M., and Alessi, D. R. (2009) Ku-0063794 is a specific inhibitor of the mammalian target of rapamycin (mTOR). *Biochem. J.* **421,** 29–42 CrossRef Medline
35. Breuleux, M., Klopfenstein, M., Stephan, C., Doughty, C. A., Barys, L., Maira, S.-M., Kwiatkowski, D., and Lane, H. A. (2009) Increased AKT Ser-473 phosphorylation after mTORC1 inhibition is rictor-dependent and does not predict tumor cell response to PI3K/mTOR inhibition. *Mol. Cancer Ther.* **8,** 742–753 CrossRef Medline
36. Rodrik-Outmezguine, V. S., Chandarlapaty, S., Pagano, N. C., Poulikakos, P. I., Scaltriti, M., Moskatel, E., Baselga, J., Guichard, S., and Rosen, N. (2011) mTOR kinase inhibition causes feedback-dependent biphasic regulation of AKT signaling. *Cancer Discov.* **1,** 248–259 CrossRef Medline
37. Neil, J., Shannon, C., Mohan, A., Laurent, D., Murali, R., and Jhanwar-Uniyal, M. (2016) ATP-site binding inhibitor effectively targets mTORC1 and mTORC2 complexes in glioblastoma. *Int. J. Oncol.* **48,** 1045–1052 CrossRef Medline
38. Manning, B. D., and Toker, A. (2017) AKT/PKB signaling: navigating the network. *Cell* **169,** 381–405 CrossRef Medline
39. Kabeya, Y., Mizushima, N., Ueno, T., Yamamoto, A., Kirisako, T., Noda, T., Kominami, E., Ohsumi, Y., and Yoshimori, T. (2000) LC3, a mamma-

lian homologue of yeast Apg8p, is localized in autophagosome membranes after processing. *EMBO J.* **19,** 5720–5728 CrossRef Medline
40. Mizushima, N., and Yoshimori, T. (2007) How to interpret LC3 immunoblotting. *Autophagy* **3,** 542–545 CrossRef Medline
41. Pugsley, H. R. (2017) Assessing autophagic flux by measuring LC3, p62, and LAMP1 co-localization using multispectral imaging flow cytometry. *J. Vis. Exp.* **125,** CrossRef Medline
42. Tanida, I., Ueno, T., and Kominami, E. (2008) LC3 and autophagy. *Methods Mol. Biol.* **445,** 77–88 CrossRef Medline
43. Schmidt, E. K., Clavarino, G., Ceppi, M., and Pierre, P. (2009) SUnSET, a nonradioactive method to monitor protein synthesis. *Nat. Methods* **6,** 275–277 CrossRef Medline
44. Chiang, G. G., and Abraham, R. T. (2005) Phosphorylation of mammalian target of rapamycin (mTOR) at Ser-2448 is mediated by p70S6 kinase. *J. Biol. Chem.* **280,** 25485–25490 CrossRef Medline
45. Mullen, R. J., Buck, C. R., and Smith, A. M. (1992) NeuN, a neuronal specific nuclear protein in vertebrates. *Development* **116,** 201–211 Medline
46. Wolf, H. K., Buslei, R., Schmidt-Kastner, R., Schmidt-Kastner, P. K., Pietsch, T., Wiestler, O. D., and Blümcke, I. (1996) NeuN: a useful neuronal marker for diagnostic histopathology. *J. Histochem. Cytochem.* **44,** 1167–1171 CrossRef Medline
47. Maximova, O. A., Murphy, B. R., and Pletnev, A. G. (2010) High-throughput automated image analysis of neuroinflammation and neurodegeneration enables quantitative assessment of virus neurovirulence. *Vaccine* **28,** 8315–8326 CrossRef Medline
48. Béïque, J.-C., and Andrade, R. (2003) PSD-95 regulates synaptic transmission and plasticity in rat cerebral cortex. *J. Physiol.* **546,** 859–867 CrossRef Medline
49. Chen, X., Nelson, C. D., Li, X., Winters, C. A., Azzam, R., Sousa, A. A., Leapman, R. D., Gainer, H., Sheng, M., and Reese, T. S. (2011) PSD-95 is required to sustain the molecular organization of the postsynaptic density. *J. Neurosci.* **31,** 6329–6338 CrossRef Medline
50. Taft, C. E., and Turrigiano, G. G. (2014) PSD-95 promotes the stabilization of young synaptic contacts. *Philos. Trans. R. Soc. Lond. B Biol. Sci.* **369,** 20130134 CrossRef Medline
51. Yoshiyama, Y., Higuchi, M., Zhang, B., Huang, S.-M., Iwata, N., Saido, T. C., Maeda, J., Suhara, T., Trojanowski, J. Q., and Lee, V. M. (2007) Synapse loss and microglial activation precede tangles in a P301S tauopathy mouse model. *Neuron* **53,** 337–351 CrossRef Medline
52. Leyns, C. E. G., Ulrich, J. D., Finn, M. B., Stewart, F. R., Koscal, L. J., Remolina Serrano, J., Robinson, G. O., Anderson, E., Colonna, M., and Holtzman, D. M. (2017) TREM2 deficiency attenuates neuroinflammation and protects against neurodegeneration in a mouse model of tauopathy. *Proc. Natl. Acad. Sci. U.S.A.* **114,** 11524–11529 CrossRef Medline
53. Cherry, J. D., Olschowka, J. A., and O'Banion, M. K. (2014) Neuroinflammation and M2 microglia: the good, the bad, and the inflamed. *J. Neuroinflamm.* **11,** 98 CrossRef Medline
54. Chesser, A. S., Pritchard, S. M., and Johnson, G. V. (2013) Tau clearance mechanisms and their possible role in the pathogenesis of Alzheimer disease. *Front. Neurol.* **4,** 122 CrossRef Medline
55. Bartaula-Brevik, S., Lindstad Brattås, M. K., Tvedt, T. H. A., Reikvam, H., and Bruserud Ø. (2018) Splenic tyrosine kinase (SYK) inhibitors and their possible use in acute myeloid leukemia. *Expert Opin. Invest. Drugs* **27,** 377–387 CrossRef Medline
56. Carnevale, J., Ross, L., Puissant, A., Banerji, V., Stone, R. M., DeAngelo, D. J., Ross, K. N., and Stegmaier, K. (2013) SYK regulates mTOR signaling in AML. *Leukemia* **27,** 2118–2128 CrossRef Medline
57. Choi, S.-H., Gonen, A., Diehl, C. J., Kim, J., Almazan, F., Witztum, J. L., and Miller, Y. I. (2015) SYK regulates macrophage MHC-II expression via activation of autophagy in response to oxidized LDL. *Autophagy* **11,** 785–795 CrossRef Medline
58. Fruchon, S., Kheirallah, S., Al Saati, T., Ysebaert, L., Laurent, C., Leseux, L., Fournié, J. J., Laurent, G., and Bezombes, C. (2012) Involvement of the Syk-mTOR pathway in follicular lymphoma cell invasion and angiogenesis. *Leukemia* **26,** 795–805 CrossRef Medline
59. Gao, P., Qiao, X., Sun, H., Huang, Y., Lin, J., Li, L., Wang, X., and Li, C. (2017) Activated spleen tyrosine kinase promotes malignant progression of oral squamous cell carcinoma via mTOR/S6 signaling pathway in an ERK1/2-independent manner. *Oncotarget* **8,** 83900–83912 CrossRef Medline
60. Krisenko, M. O., Higgins, R. L., Ghosh, S., Zhou, Q., Trybula, J. S., Wang, W.-H., and Geahlen, R. L. (2015) Syk is recruited to stress granules and promotes their clearance through autophagy. *J. Biol. Chem.* **290,** 27803–27815 CrossRef Medline
61. Leseux, L., Hamdi, S. M., Al Saati, T., Capilla, F., Recher, C., Laurent, G., and Bezombes, C. (2006) Syk-dependent mTOR activation in follicular lymphoma cells. *Blood* **108,** 4156–4162 CrossRef Medline
62. Cuervo, A. M. (2008) Autophagy and aging: keeping that old broom working. *Trends Genet.* **24,** 604–612 CrossRef Medline
63. Eskelinen, E.-L., and Saftig, P. (2009) Autophagy: a lysosomal degradation pathway with a central role in health and disease. *Biochim. Biophys. Acta* **1793,** 664–673 CrossRef Medline
64. Funderburk, S. F., Marcellino, B. K., and Yue, Z. (2010) Cell "self-eating" (autophagy) mechanism in Alzheimer's disease. *Mt. Sinai J. Med.* **77,** 59–68 CrossRef Medline
65. Lee, J.-H., Yu, W. H., Kumar, A., Lee, S., Mohan, P. S., Peterhoff, C. M., Wolfe, D. M., Martinez-Vicente, M., Massey, A. C., Sovak, G., Uchiyama, Y., Westaway, D., Cuervo, A. M., and Nixon, R. A. (2010) Lysosomal proteolysis and autophagy require presenilin 1 and are disrupted by Alzheimer-related PS1 mutations. *Cell* **141,** 1146–1158 CrossRef Medline
66. Fatouros, C., Pir, G. J., Biernat, J., Koushika, S. P., Mandelkow, E., Mandelkow, E.-M., Schmidt, E., and Baumeister, R. (2012) Inhibition of tau aggregation in a novel *Caenorhabditis elegans* model of tauopathy mitigates proteotoxicity. *Hum. Mol. Genet.* **21,** 3587–3603 CrossRef Medline
67. Yanamandra, K., Jiang, H., Mahan, T. E., Maloney, S. E., Wozniak, D. F., Diamond, M. I., and Holtzman, D. M. (2015) Anti-tau antibody reduces insoluble tau and decreases brain atrophy. *Ann. Clin. Transl. Neurol.* **2,** 278–288 CrossRef Medline
68. Kimura, T., Fukuda, T., Sahara, N., Yamashita, S., Murayama, M., Mizoroki, T., Yoshiike, Y., Lee, B., Sotiropoulos, I., Maeda, S., and Takashima, A. (2010) Aggregation of detergent-insoluble tau is involved in neuronal loss but not in synaptic loss. *J. Biol. Chem.* **285,** 38692–38699 CrossRef Medline
69. Bellucci, A., Westwood, A. J., Ingram, E., Casamenti, F., Goedert, M., and Spillantini, M. G. (2004) Induction of inflammatory mediators and microglial activation in mice transgenic for mutant human P301S tau protein. *Am. J. Pathol.* **165,** 1643–1652 CrossRef Medline
70. Korzhevskii, D. E., and Kirik, O. V. (2016) Brain microglia and microglial markers. *Neurosci. Behav. Physi.* **46,** 284 CrossRef
71. Xu, N., Tang, X.-H., Pan, W., Xie, Z.-M., Zhang, G.-F., Ji, M.-H., Yang, J.-J., Zhou, M.-T., and Zhou, Z.-Q. (2017) Spared nerve injury increases the expression of microglia M1 markers in the prefrontal cortex of rats and provokes depression-like behaviors. *Front. Neurosci.* **11,** 209 CrossRef Medline
72. Sofroniew, M. V., and Vinters, H. V. (2010) Astrocytes: biology and pathology. *Acta Neuropathol.* **119,** 7–35 CrossRef Medline
73. von Bernhardi, R., Tichauer, J. E., and Eugenín, J. (2010) Aging-dependent changes of microglial cells and their relevance for neurodegenerative disorders. *J. Neurochem.* **112,** 1099–1114 CrossRef Medline
74. Wang, W.-Y., Tan, M.-S., Yu, J.-T., and Tan, L. (2015) Role of pro-inflammatory cytokines released from microglia in Alzheimer's disease. *Ann. Transl. Med.* **3,** 136 CrossRef Medline
75. Srivastava, I. N., Shperdheja, J., Baybis, M., Ferguson, T., and Crino, P. B. (2016) mTOR pathway inhibition prevents neuroinflammation and neuronal death in a mouse model of cerebral palsy. *Neurobiol. Dis.* **85,** 144–154 CrossRef Medline
76. Zheng, H.-F., Yang, Y.-P., Hu, L.-F., Wang, M.-X., Wang, F., Cao, L.-D., Li, D., Mao, C.-J., Xiong, K.-P., Wang, J.-D., and Liu, C.-F. (2013) Autophagic impairment contributes to systemic inflammation-induced dopaminergic neuron loss in the midbrain. *PLoS One* **8,** e70472 CrossRef Medline
77. Zhou, X., Zhou, J., Li, X., Guo, C., Fang, T., and Chen, Z. (2011) GSK-3β inhibitors suppressed neuroinflammation in rat cortex by activating autophagy in ischemic brain injury. *Biochem. Biophys. Res. Commun.* **411,** 271–275 CrossRef Medline

78. Alirezaei, M., Kiosses, W. B., Flynn, C. T., Brady, N. R., and Fox, H. S. (2008) Disruption of neuronal autophagy by infected microglia results in neurodegeneration. *PLoS One* **3,** e2906 CrossRef Medline
79. Bain, H. D. C., Davidson, Y. S., Robinson, A. C., Ryan, S., Rollinson, S., Richardson, A., Jones, M., Snowden, J. S., Pickering-Brown, S., and Mann, D. M. A. (2019) The role of lysosomes and autophagosomes in frontotemporal lobar degeneration. *Neuropathol. Appl. Neurobiol.* **45,** 244–261 CrossRef Medline
80. Yura, T., Concepcion, A. B., Han, G., Hiraoka, M., Katsumata, H., Kawamura, N., Kokubo, T., Komura, H., Li, Y., Lowinger, T., Mogi, M., Yamamoto, N., Yoshida, N., *et. al.* (November 08, 2001) U.S. Patent WO/2001/083485A1
81. Fernández-Nogales, M., Cabrera, J. R., Santos-Galindo, M., Hoozemans, J. J. M., Ferrer, I., Rozemuller, A. J., Hernández, F., Avila, J., and Lucas, J. J. (2014) Huntington's disease is a four-repeat tauopathy with tau nuclear rods. *Nat. Med* **20,** 881–885 CrossRef Medline
82. Sarkar, S. (2013) Regulation of autophagy by mTOR-dependent and mTOR-independent pathways: autophagy dysfunction in neurodegenerative diseases and therapeutic application of autophagy enhancers. *Biochem. Soc. Trans.* **41,** 1103–1130 CrossRef Medline